

Review

Synthesis and Applications of Dimensional SnS₂ and SnS₂/Carbon Nanomaterials

Catherine Sekyerebea Diko¹, Maurice Abitonze¹ , Yining Liu¹, Yimin Zhu^{1,*} and Yan Yang^{2,*}¹ College of Environmental Science and Engineering, Dalian Maritime University, Dalian 116026, China² Dalian Research Institute of Petroleum and Petrochemicals, SINOPEC, Dalian 116045, China

* Correspondence: ntp@dmlu.edu.cn (Y.Z.); yangyan.fshy@sinopec.com (Y.Y.)

Abstract: Dimensional nanomaterials can offer enhanced application properties benefiting from their sizes and morphological orientations. Tin disulfide (SnS₂) and carbon are typical sources of dimensional nanomaterials. SnS₂ is a semiconductor with visible light adsorption properties and has shown high energy density and long cycle life in energy storage processes. The integration of SnS₂ and carbon materials has shown enhanced visible light absorption and electron transmission efficiency. This helps to alleviate the volume expansion of SnS₂ which is a limitation during energy storage processes and provides a favorable bandgap in photocatalytic degradation. Several innovative approaches have been geared toward controlling the size, shape, and hybridization of SnS₂/Carbon composite nanostructures. However, dimensional nanomaterials of SnS₂ and SnS₂/Carbon have rarely been discussed. This review summarizes the synthesis methods of zero-, one-, two-, and three-dimensional SnS₂ and SnS₂/Carbon composite nanomaterials through wet and solid-state synthesis strategies. Moreover, the unique properties that promote their advances in photocatalysis and energy conversion and storage are discussed. Finally, some remarks and perspectives on the challenges and opportunities for exploring advanced SnS₂/Carbon nanomaterials are presented.

Keywords: tin disulfide; carbon materials; composite nanomaterials; photocatalysis; energy storage batteries



Citation: Diko, C.S.; Abitonze, M.; Liu, Y.; Zhu, Y.; Yang, Y. Synthesis and Applications of Dimensional SnS₂ and SnS₂/Carbon Nanomaterials. *Nanomaterials* **2022**, *12*, 4497. <https://doi.org/10.3390/nano12244497>

Academic Editor: Vincenzo Vaiano

Received: 3 December 2022

Accepted: 14 December 2022

Published: 19 December 2022

Publisher's Note: MDPI stays neutral with regard to jurisdictional claims in published maps and institutional affiliations.



Copyright: © 2022 by the authors. Licensee MDPI, Basel, Switzerland. This article is an open access article distributed under the terms and conditions of the Creative Commons Attribution (CC BY) license (<https://creativecommons.org/licenses/by/4.0/>).

1. Introduction

The fast depletion of fossil fuel and its environmental implications have led to the development of technologies for green-energy production and storage as well as environmental remediation. These technologies are of great interest to the research community to minimize carbon footprints. Therefore, breakthroughs in nanotechnology research could enable the creation of unique materials at the molecular level, opening up a slew of green industrial possibilities.

Dimensional nanomaterials have become a trendy topic in recent years and have aroused tremendous research interest due to their unique physicochemical and structural properties [1–3]. These dimensional nanomaterials have integrated architectures that exhibit well-oriented dimensions of zero-, one-, two-, or three-dimensional (0D, 1D, 2D, 3D) architectures, such as quantum dots, nanofibers, nanorods, nanowires, nanosheets, nanoflowers, and nanospheres [4–6]. This development has allowed for diverse applications in catalysis, optoelectronics, and electronic devices [7,8].

SnS₂ nanomaterials have made impactful strides in the synthesis of dimensional nanomaterials, due to their unique hexagonal nanostructures and the ability to have sulfur chains with variable lengths. In addition, SnS₂ has a favorable energy bandgap, low cost, low toxicity, excellent stability, and abundant reserves in nature. However, its wide application in batteries is hindered by low intrinsic conductivity and poor cycling stability [9,10]. One of the most effective techniques used to tackle these problems is the synthesis of SnS₂ in composite nanomaterials. Carbon materials are economically abundant and have

presented numerous advantages because of their unique physio-chemical and electrochemical properties, such as a high specific surface area, outstanding electrical and mechanical properties, and narrowing bandgap effect [11–14]. This makes carbon materials a great candidate to be used as a hybrid material. At the nano level, carbon materials offer a diversity of morphologies and structures (e.g., quantum dots, nanotubes, nanowire, graphene, nanospheres, graphene oxide, etc.), each of which is unique to its respective application technology [15–19]. The characteristic properties of composite nanostructures are inherited from the individual precursor components, leading to dimensionally synthesized hybrid architectures that are fit for various applications [20–25]. Moreover, the synergistic features of these functional nanocomposites can be achieved through the manipulation of their dimensions during synthesis. Therefore, a combination of SnS₂ and carbon materials can lead to integrated SnS₂/Carbon nanomaterials with enhanced properties in photocatalysis, electrochemical conversion, and energy storage applications.

Progress has been made in the synthesis and applications of SnS₂ nanomaterials using wet and solid-phase synthesis methods [26–28]. In the last five years, a number of exciting reviews on SnS₂ have been published, focused on preparation, microstructure characterization methods, and application [29,30]. However, a focus on dimensional SnS₂ nanocomposite architectures has not yet been reported. With the growing number of publications on SnS₂ composite nanomaterials, there is a need to present an updated review article on the state-of-the-art development of SnS₂/Carbon composites at the nano dimensional level. This review thus aims to give an overview of the progress made in the synthesis, dimensional characterization, and applications of SnS₂/Carbon nanomaterials. SnS₂ and SnS₂/Carbon nanomaterials have some similarities in synthesis methods and application fields. So, the synthesis of SnS₂ nanomaterials was first presented in this review for an overview of the fabrication methods, followed by SnS₂/Carbon composite nanomaterials. The various nanostructural architectures were dimensionally classified in terms of zero, one, two, and three dimensions (0D, 1D, 2D, and 3D). Furthermore, this review examines the advances in the development of SnS₂/Carbon hybrid nanomaterials in photocatalysis as well as electrochemical energy conversion and storage applications.

This review adopted a scoping review approach because it offers qualitative and quantitative opportunities to identify the scope of a body of literature relating to a particular topic, identify and clarify concepts associated with the research topic, and understand the research methods associated with the research topic [31]. The review used articles sourced from the Web of Science database starting with the keywords “SnS₂”, “Tin disulfide”, “carbon”, “photocatal*”, and “battery*”. These were further enhanced by an iterative process of searching for articles around the three main focal areas that underpin this research, namely (i) synthesis, (ii) dimensional characteristics, and (iii) applications of synthesized material. This in turn became part of the criteria for selecting articles to be reviewed. In addition, all articles used were peer-review articles to ensure that the findings that are included in this review were based on sound science. Each article was reviewed to provide inputs for the three focal areas of this research. This subsequently informed the themes or categories which formed the sub-focal areas for this review. In situations where new themes were emerging, but the search did not capture more publications, further search was conducted. For instance, to identify additional and specific concepts related to the synthesis method, keywords such as wet or solid-state synthesis were applied to capture additional publications. This was the same when choosing articles with different morphological dimensions. As a result, there is no specific count of articles for each search and inclusion, which is typical of a scoping review.

2. Synthesis Methods

2.1. Wet Chemical Synthesis of SnS₂ and SnS₂/Carbon Nanomaterials

Wet chemical syntheses of nanomaterials involve chemical reactions in the solution phase using precursors at suitable experimental conditions. The synthesis technique varies depending on the solvent medium used. The wet chemical synthesis approach is a bottom-

up method; as such, it offers a high degree of controlling and fabricating nanomaterials. Hydrothermal synthesis, [32,33] solvothermal synthesis, [34,35] template synthesis, [36] self-assembly, [37] hot-injection [38], and interface-mediated synthesis [39] all fall under wet-chemical synthesis routes. Amongst these, hydrothermal and solvothermal approaches are easy and reproducible methods and have been widely adapted for the preparation of inorganic nanomaterials.

2.1.1. Wet Chemical Synthesis of SnS₂ Nanomaterials

Several synthesis strategies have been reported, and new ones are being discovered to fabricate and better understand nanostructures of SnS₂ nanomaterials. Through wet-chemical synthesis, Chaki et al. achieved 0D semiconductor SnS₂ nanoparticles synthesized at room temperature using Tin(IV) chloride pentahydrate (SnCl₄·5H₂O) and thioacetamide (C₂H₅NS) as precursors [40]. Hexagonal crystal structures of SnS₂ nanoparticles were also synthesized in a similar fashion without the addition of any surfactants or needing further purification [41].

As a typical wet-chemical synthesis method, hydrothermal treatment has often been used in the synthesis of SnS₂. V-doped binary SnS₂ buffer layers and SnS₂ nanoflakes were prepared hydrothermally [42–44]. The obtained porous structures were interconnected with each other, displaying a high surface area. In other studies, using the solvothermal route, SnS₂ nanomaterials were fabricated with different types of solvents [45,46]. This method has been used to achieve sheet-like, flower-like, and ellipsoid-like SnS₂ nanostructures as potential electrode material [47]. The influence of thiourea concentration, solvent system, and reaction time have been proposed as vital in the solvothermal synthesis method. Wang et al. also added that high-boiling-point and low-viscosity solvents are needed for the reaction and product separation [48]. As such, the system can provide suitable surface energy that could effectively stabilize their 2D structures and suppress nanomaterials from further aggregation. In addition, using surfactants is a typical way to adjust the surface energy; as such, Triton X-100 was used, which played a crucial role in controlling the morphology of hexagonal SnS₂ nanoflakes [49].

Chemical vapor deposition (CVD) and the high-temperature hot injection method have also been successfully used to fabricate SnS₂ nanostructures composed of vertically oriented 2D sheet arrays with high crystallinity and single-phased SnS₂ nanosheets, respectively [50,51]. Solvents and precursors play important roles in catalyzing and increasing the kinetics of a reaction. Thus, for the controlled synthesis of nanomaterials, the focus should not only be on their fundamental shape or size-dependent properties and technological applications but also on the synthesis and assembly properties [52]. Another unique process was illustrated by Jana et al., using ionothermal synthesis to achieve SnS₂ nanoflowers at low and high temperatures with exceptional nanostructures as depicted in Figure 1a [53]. The crystal structures of the synthesized nanostructures were determined by XRD analysis, highlighting the hexagonal SnS₂ structures with (001) and (101) crystallographic planes (Figure 1b). This hexagonal nature is common in SnS₂ and composite associations. The medium for synthesis was water-soluble ionic liquids. The ionic liquid served as a template at a low temperature to achieve the hierarchical layered polycrystalline 2D SnS₂ nanosheet petals. These were combined by the effects of hydrogen bonding, imidazolium stacking, and electrostatic and hydrophobic interactions. On the other hand, a high-temperature reaction yielded plate-like nanosheets with well-defined crystallographic facets because of the rapid inter-particle diffusion across the ionic liquid. The various synthesis processes of SnS₂ nanomaterials have allowed the integration of diverse hybrid materials to enhance their application properties.

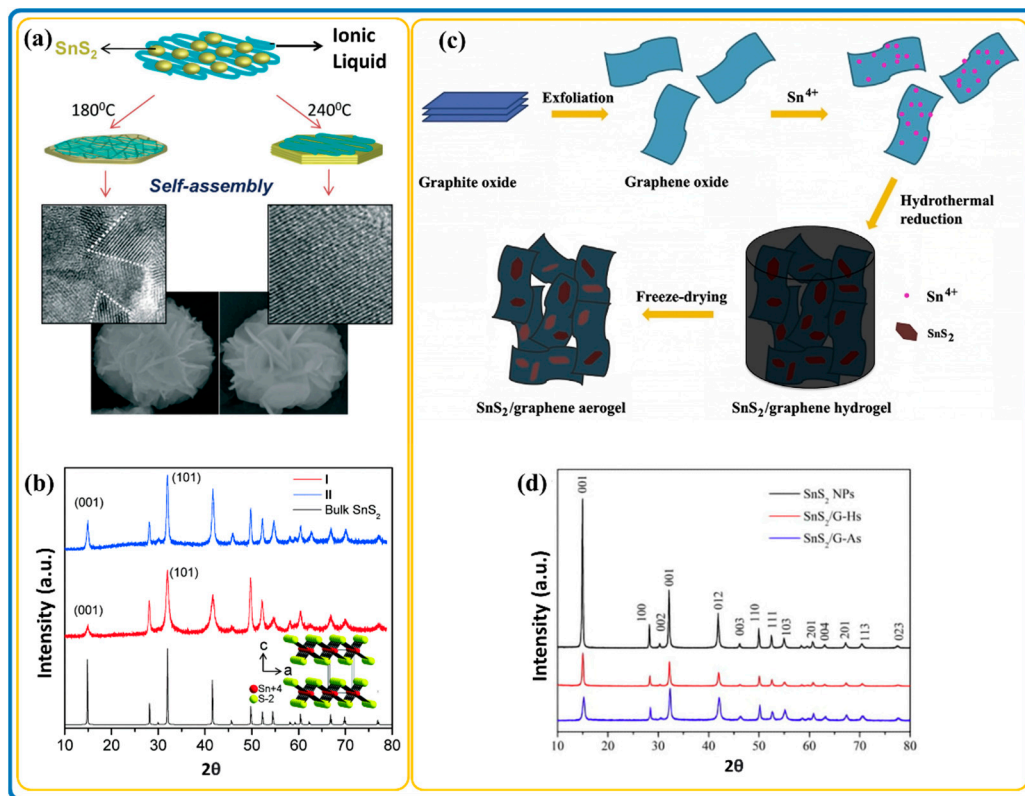


Figure 1. (a) Schematic illustration of ionothermal assembly (b) X-ray diffraction (XRD), of SnS₂ flowers at lower and higher temperatures. Adapted with permission from [53]. Copyright 2014, Elsevier. (c) Self-assembly synthesis process (d) XRD, of 3D SnS₂/Graphene aerogels. Adapted with permission from [54]. Copyright 2013, Elsevier.

2.1.2. Wet Chemical Synthesis of SnS₂/Carbon Nanomaterials

Just like SnS₂ nanomaterials, the structure of SnS₂/carbon composite nanomaterials depends on the precursors and the synthesis conditions. Normally, SnS₂/carbon composites result in different dimensional architectures, where the SnS₂ nanostructures anchor themselves onto interpenetrated carbon materials with varied architectures. Figure 1c is a clear representation of self-assembled SnS₂/carbon composite nanostructures. It shows 3D SnS₂/graphene aerogel nanostructures fabricated through in situ macroscopy self-assembly using a hydrothermal process, followed by freeze-drying to preserve its 3D architectures. Figure 1d shows the crystalline structure of SnS₂ in composite materials; however, it could not detect the carbon peaks due to its amorphous form. For that matter, Raman spectroscopy was proposed for the detection of carbon in the composite.

Controlling the growth orientations of SnS₂ nanostructures on nanocarbon surfaces has been reported as a challenging concept as seen in the fabrication of parallel and vertically aligned SnS₂ nanostructures on graphene nanosheets [55]. Hence, an understanding of the mechanism of SnS₂/carbon hybrid synthesis, with desired properties and varied nanostructures, is important in nanotechnological applications. Liu et al. synthesized SnS₂/bacterial-cellulose-derived carbon nanofiber (BC-CNF) first by the hydrolysis of thioacetamide, followed by in situ metathesis reactions, and finally by self-assembly and oriented crystallization processes [56]. The resultant BC-CNFs had a highly porous 3D network with an average diameter of 30–50 nm. Among the methods adopted for synthesizing SnS₂/Carbon nanomaterials, the most prevalent is the hydrothermal process. This technique can enhance the characteristics and stability of nanomaterials while concurrently controlling the structures of the hybrid composites. These allow for interconnected networks with a high surface area which enhances the synergetic interactions between the layered SnS₂ and the carbon by increasing their contact areas [57]. Furthermore, the

interconnected network helps SnS₂ in alleviating the mechanical stress, preventing its aggregation, and accommodating its volume change during cycling [58,59]. For instance, SnS₂/graphene oxide nanocomposites were synthesized by reflux condensation together with a hydrothermal strategy using an anionic surfactant, sodium dodecyl sulfate (SDS) [60]. Zhang et al. also proposed a means for fabricating hierarchical polyaniline/SnS₂@carbon nanotubes onto the carbon fiber (CF) surface [61]. However, synthesis limitations, such as low pressure and temperature can seriously affect the rate performance of composite materials [62,63].

Solvothermal synthesis has been used to investigate the synthesis of SnS₂/carbon composite nanomaterials, but only a handful of reports exist on the use of this method. For example, Zhang et al. synthesized one-pot flexible SnS₂/CNT (2D nanosheet/3D self-assembled flower) composites which were controlled by a time-dependent process [64]. Moreover, functionalized graphene sheets (FGS) were used to synthesize graphene-SnS₂ nanocomposites via a solvothermal method [65]. In most cases, annealing is used for further treatment to improve the phase purity and crystallinity of nanomaterials before use in various applications [10,66].

2.2. Solid-Phase Synthesis of SnS₂ and SnS₂/Carbon Nanomaterials

Solid-phase synthesis is a top-down approach to synthesizing inorganic nanomaterials. The procedure involves milling and may include many annealing steps with several intermediate milling procedures to heighten the uniformity of the mixture and reduce the sizes of the fabricated materials [67–71]. Additional milling tends to make the particles more sinter active in the heat treatment procedures that follow [72,73]. Furthermore, huge quantities of materials can be synthesized in a reasonably straightforward method, but the resulting nanomaterials have a comparatively high agglomeration compared to the wet synthesis processes discussed above [74,75]. As a result, solid-phase synthesis produces relatively large particle sizes and poor homogeneity which are somewhat unavoidable.

2.2.1. Solid-Phase Synthesis of SnS₂ Nanomaterials

Solid-phase synthesis of SnS₂ nanomaterials is an alternative fabrication method that helps the growth of SnS₂ nanostructures by supplying an adequate amount of precursors [76]. Usually, this is carried out without the aid of a template, inert gas protection, or a vacuum environment but by heating the solid precursor mixtures in air at certain temperatures and time followed by washing treatment [77]. In some reports, SnS₂ nanoflakes were fabricated using a suitable amount of SnCl₄·5H₂O and thiourea mixed and grounded thoroughly until a homogeneous mixture was acquired and subsequently heated in a crucible [78,79]. Owing to the intrinsic anisotropic nature of SnS₂ crystals, solid-phase synthesis tries to enhance its surface area to achieve desired nanostructures through the milling process. Xiao et al. and Wang et al. prepared SnS₂ nanomaterials by heating the precursors at their liquid–solid phase, i.e., at the melting points and boiling points of tin (Sn), sulfur (S), and ammonium chloride (NH₄Cl) in air [80,81]. In addition, the presence of NH₄Cl aided and promoted the synthesis of pure SnS₂ under mild conditions. It is worth noting that the annealing process of nanomaterials can also bring about self-purification due to the impurities and intrinsic material defects that prefer moving toward the surface during the annealing process.

2.2.2. Solid-Phase Synthesis of SnS₂/Carbon Nanomaterials

To the best of our knowledge, limited literature exists on the solid-state synthesis of SnS₂/Carbon nanomaterials. The solid synthesis of SnS₂/Carbon nanomaterials may involve microwave heating, calcination, milling, or a combination of these processes to achieve a homogeneous crystalline product. The mechanical energy used creates phase transformations and chemical reactions at very low temperatures. For instance, ball milling enables the reduction in particle sizes and characteristic lengths in addition to the effective mutual dispersion of the processed phases. Wang et al. synthesized a SnS₂/Carbon compos-

ite by annealing metallic Sn, S powder, and polyacrylonitrile (PAN) mixed in a sealed glass tube under vacuum at 600 °C for 3 h [82]. This resulted in SnS₂ nanostructures embedded in the carbon matrix that was generated by the carbonization of PAN. The morphologies are shown in Figure 2a and the synthesis process is schematically shown in Figure 2b. Furthermore, the synthesized SnS₂/carbon composite was directly milled in NaCl which reduced the crystal structure of the SnS₂/Carbon nanocomposite, and this improved the overall battery performance of the synthesized SnS₂/Carbon nanomaterial [83]. Figure 2c shows the SEM of un-milled and directly milled SnS₂/Carbon structures, respectively and Figure 2d shows the schematic formation of SnS₂/Carbon composite.

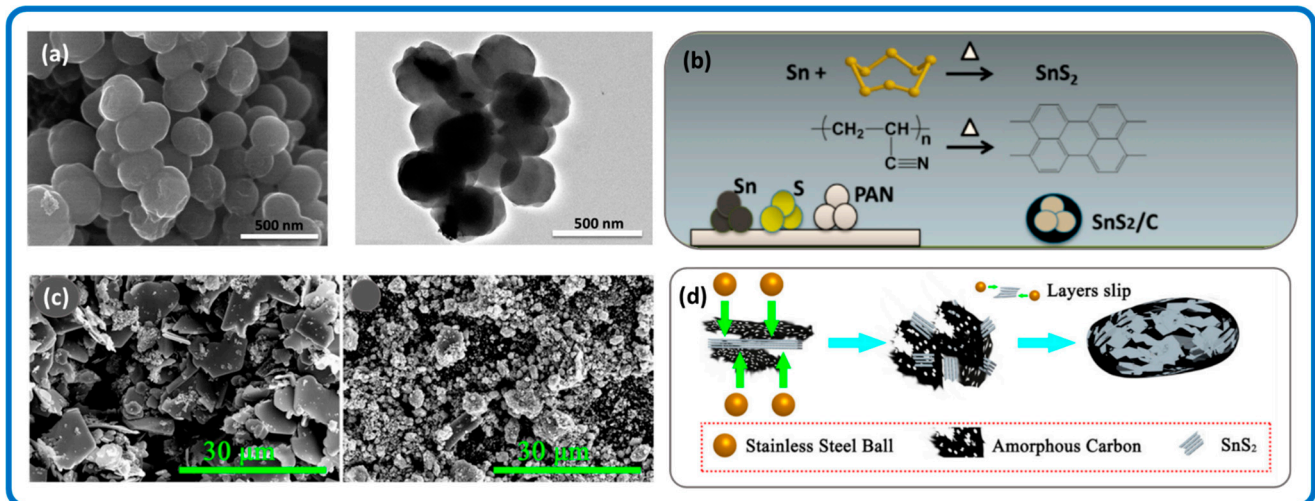


Figure 2. (a) SEM and TEM images, (b) Schematic illustration of solid-state synthesis route, of SnS₂/carbon nanomaterials. Adapted with permission from [82]. Copyright 2015, American Chemical Society. (c) SEM images of un-milled and directly milled SnS₂/Carbon. (d) Schematic illustration of ball milling of SnS₂/carbon to decrease its crystallinity. Reprinted with permission from Springer Nature from [83]. Copyright 2016, Elsevier.

In some other processes, solid-state synthesis has been indicated to require low temperatures and help to improve the purity of the resultant substances [84,85]. The solid-state syntheses have also been applied in the synthesis of other SnS₂/composites including Phosphorus-SnS₂ composites, which is not the focus of this review [86]. Figure 3a demonstrates the simple synthesis routes of SnS₂/Carbon nanomaterials by wet chemical and Figure 3b by solid-state synthesis. Table 1 shows the various SnS₂/Carbon nanomaterials achieved through wet and solid-state synthesis approaches. In other instances, a hybrid synthesis method was employed to achieve SnS₂/carbon composite nanomaterials [87,88]. In one instance, the carbon precursor was synthesized at elevated temperatures before it was further combined with the Sn²⁺ and S²⁻ precursors to form the composite SnS₂/carbon nanomaterials [89,90].

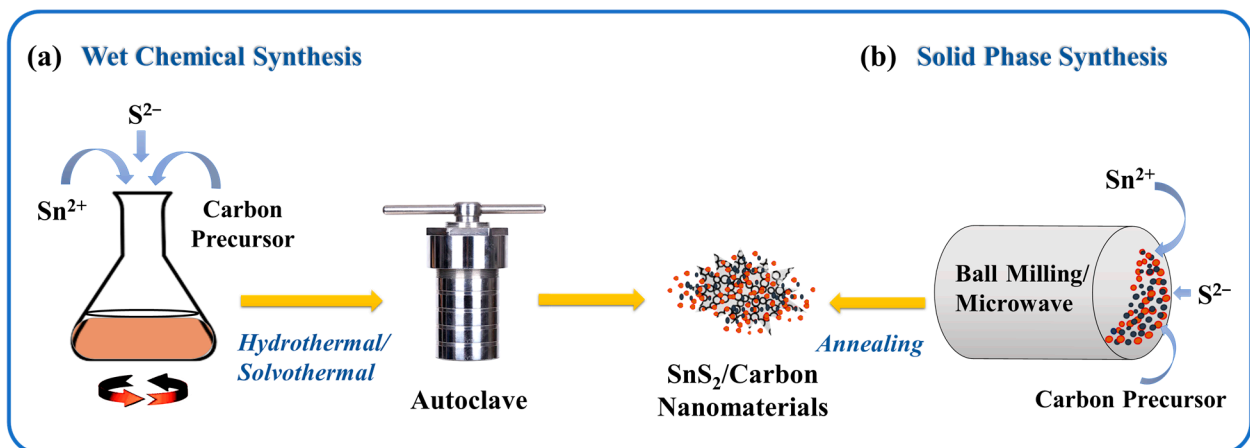


Figure 3. (a) Schematic illustration of wet chemical synthesis and (b) solid-state synthesis route of SnS₂ and SnS₂/Carbon nanomaterials.

Table 1. Comparison of the various SnS₂/Carbon nanomaterials achieved through wet and solid-state synthesis approaches and their applications.

Dimension	Synthesis Method	SnS ₂ /Carbon Composites	Applications	Ref.
0D	Solid-State Synthesis	SnS ₂ /Fullerene	-	[91]
1D	Facile Electrospinning Technique	SnS ₂ / NSDC ¹ Nanofibers	SIBs ²	[92]
	Hydrothermal Method	Polypyrrole@SnS ₂ @Carbon Nanofiber	LIBs ³	[93]
	Facile Sintering Route	SnS ₂ Cross-Linked/ CNTs ⁴	SIBs	[94]
	Solvothermal Method	SnS ₂ Nanoflakes/CNT	LIBs	[95]
	Hydrothermal Method	SnS ₂ @rGF ⁵	SIBs	[96]
	Plasma Evaporation and Post Sulfurization	SnS ₂ Semi-Filled CNT	LIBs	[97]
2D	Hydrothermal Method	SnS ₂ /rGO ⁶	LIBs	[98]
	Hydrothermal Method	SnS ₂ /Graphene Aerogel	SIBs	[99]
	Hydrothermal Method	SnS ₂ /Graphene	SIBs	[100]
	Thermal Annealing	SnS ₂ /rGO	SIBs	[101]
	Ultrasonication	SnS ₂ /Graphene	LIBs/ SIBs	[102]
	Hydrothermal Method	Carbon-Doped SnS ₂	CO ₂ Reduction in Fuel Cell	[103]
	Solvothermal Method	SnO ₂ -rGO/SnS ₂	NO ₂ detection	[104]
	Thermal Annealing	SnS ₂ /N-Doped rGO	LIBs	[105]
Wet Chemical Transfer Method	Graphene/SnS ₂ Heterojunction	Photoelectric Performance	[106]	
3D	Solvothermal Method	SnS ₂ /GO Nanoflower	Ultrasensitive Humidity Sensor	[107]
	Hydrothermal Method	SnS ₂ /Graphene Monolith	SIBs	[108]
	Thermally Annealing	SnS ₂ /N-Doped Cubic-Like Carbon	LIBs	[109]
	Solvothermal Method	SnS ₂ /Carbon Yolk-Shell	SIBs	[110]
	Hydrothermal Method	SnS ₂ Flowers/Carbon Nanotubes	SIBs	[111]
	Hydrothermal Method	SnS ₂ @Carbon Hollow Nanospheres	SIBs	[112]
	Hydrothermal Method	SnS ₂ /rGO Spheres	Asymmetric Supercapacitors	[113]
	Hydrothermal Method	SnS ₂ /g-C ₃ N ₄ ⁷ Amorphous Spheres	Supercapacitors	[114]

¹ NSDC, Nitrogen, Sulfur-doped carbon nanofibers; ² SIBs, Sodium ion batteries; ³ LIBs, Lithium ion batteries; ⁴ CNT, Carbon nanotube; ⁵ GF, Graphene fiber; ⁶ rGO, Reduced graphene oxide; ⁷ g-C₃N₄, graphitic carbon nitride.

3. Dimensional Characteristics of SnS₂ and SnS₂/Carbon Nanomaterials

Nanomaterials possess a variety of shapes and sizes. In some cases, their names are generated and characterized by their shapes or orientations. For example, nanospheres are spherical, nanotubes are tube-shaped, etc. Nanostructure classifications are also based on their dimensions, compositions, uniformity, and agglomeration. Classification based on dimensionality is a generalization of the concept based on the aspect ratio of 0D, 1D, 2D, or 3D. These dimensions or morphologies result from a variety of precursors, temperature, pH, templates, the mode of reagent dosage during synthesis, etc. The ability to control the morphology of nanomaterials is crucial in exploiting their properties for applications. As a measure of the dimensional characteristics of SnS₂ and SnS₂/Carbon nanomaterials in this review article, TEM and SEM analyses were mainly used.

3.1. Dimensional Characteristics of SnS₂ Nanomaterials

3.1.1. Zero-Dimensional (0D Nanodots) SnS₂ Nanomaterials

SnS₂ quantum dots (QDs) possess strong luminescence, good aqueous stability, and biocompatibility. Therefore they are often used in the field of sensing and biology [115]. Excitation and emission properties exhibited by SnS₂ QDs were credited to the polydispersity of SnS₂-QDs and its characteristic feature of quantum confinement and edge effects [116]. Negatively charged SnS₂ QDs were made by inserting electrons into vacant molecular orbitals, whereas positively charged SnS₂ QDs were made by injecting holes into the highest occupied molecular orbitals, and these collided with the stable SnS₂ QDs to produce excited SnS₂ QDs that could emit light [117]. Figure 4a–d show representative transmission electron microscopy (TEM) and high-resolution transmission electron microscopy (HRTEM) details of SnS₂ QDs. Figure 4a,b are nearly monodispersed SnS₂ QDs with a mean size of 6.5 nm. A single particle lattice spacing of 0.32 nm is seen in Figure 4d corresponding to the (200) plane of hexagonal SnS₂ [118].

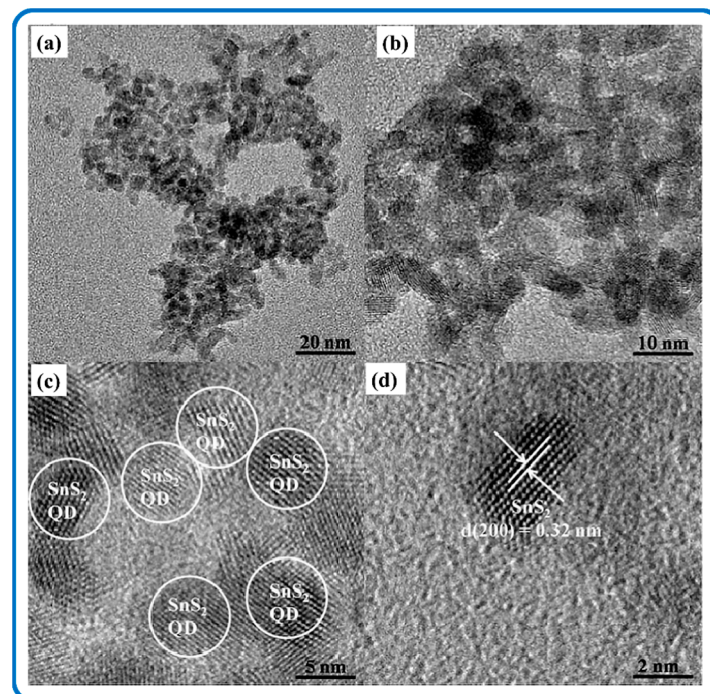


Figure 4. TEM images of SnS₂ QDs (a,b); HR-TEM images of SnS₂ QDs (c,d). Reproduced with permission from [118]. Copyright 2016, Elsevier.

The surface energy and crystal structures of the SnS₂ QDs are dependent on synthesis conditions. Optimized synthesis conditions could result in a significant increase in the surface-to-volume ratio and influence the surface energy and phase stability greatly. Hy-

drothermally synthesized SnS₂ QDs are in situ functionalized and pH sensitive [115,119]. In application, these nanomaterials can connect and partly fuse to adjacent ones leading to much flatter structures after annealing. In the end, this is valuable to form good contact between the active layer and the electrode material [120].

3.1.2. One-Dimensional (1D) SnS₂ Nanomaterials

One-dimensional nanostructures are of interest due to their potential to serve as the basis for determining the size and dimensionality dependence of a material's physical properties. Many solid structures of chalcogenide grow from 1D nanostructures. One-dimensional nanomaterials have been exploited as a novel model while investigating the size and dimensional dependence of functional properties. They also play an important role as interconnected nanostructures and as the key units in fabricating electronic, optoelectronic, and electrochemical energy devices with nanoscale dimensions. SnS₂ nanowires were synthesized by sulfurizing the Sn nanowires, which were embedded in the nanochannels of anodic aluminum oxide (AAO) templates. The characterization of these nanowires is shown in Figure 5 [121]. After detaching from the AAO templates, SnS₂ nanowires achieved a diameter of about 40 nm. It is worth noting that reports on the synthesis of 1D nanomaterial are rare, owing to the fact that most synthesized SnS₂ nanomaterials are the building blocks for achieving other dimensionally structured nanomaterials.

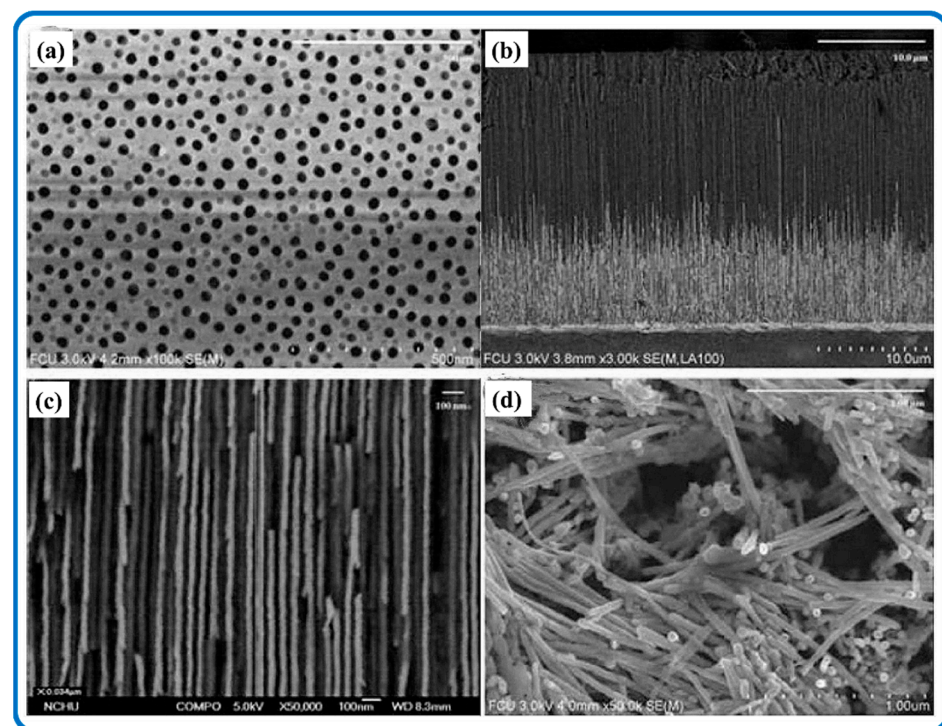


Figure 5. Field Emission Scanning Electron Microscope (FE-SEM) micrographs of (a) top view of the AAO templates for SnS₂ nanowire formation, (b) cross-section view of SnS₂ nanowires embedded in an AAO template, (c) the magnified FE-SEM micrograph of SnS₂ nanowires, and (d) SnS₂ nanowires detached from the AAO templates. Reproduced from [121]. 2009, Springer. CC BY 2.0.

3.1.3. Two-Dimensional (2D) SnS₂/Flake Nanomaterials

Researchers have made significant advances in the preparation, characterization, adjustment, and theoretical investigation of 2D materials. The abundance of 2D materials has elevated them with a range of material frameworks in methodological studies for the development of nano- and atomic-level applications. Two-dimensional SnS₂ nanocrystals exhibit semiconductor characteristics, [122] owing to their high carrier movement and large bandgap [123]. SnS₂ has a sandwich-like structure with an S plane held in between two Sn

planes, all in hexagonal order. The adjacent sulfur atoms in the sulfur layers are bonded, allowing for easy layer separation via chemical or mechanical exfoliation [41]. However, vacancy defects in 2D SnS₂ nanomaterials are known to have a major influence on material characteristics and are unavoidable during exfoliation [124]. Sun et al. confirmed the formation of micrometer-sized SnS₂ nanosheets with exposed (011) facets as the primary surfaces [125]. These 2D nanosheets could be reconstructed by lateral confinement with longitudinal extension, and a typical 2D SnS₂ structure is displayed in Figure 6. The as-grown SnS₂ nanosheets were quasi-vertically oriented and standing free on the fluorine-doped tin oxide (FTO) substrate (Figure 6a–c). The SnS₂ nanostructures displayed a well-defined semi-hexagonal shape. Similarly, Li et al. achieved 2D SnS₂ nanoflakes grown perpendicular to the substrate in a low-temperature zone of a SiO₂/Si substrate [123]. Strong light absorption, short minority-carrier transport distances, and a wide exposed surface area for catalytic reactions have all helped 2D SnS₂ nanomaterials to effectively harvest photocurrent [50]. Furthermore, 2D SnS₂ with characteristics such as mono-dispersity, high compactness, open morphology, well-defined structures, and maximally exposed surfaces/edges are favorable [51].

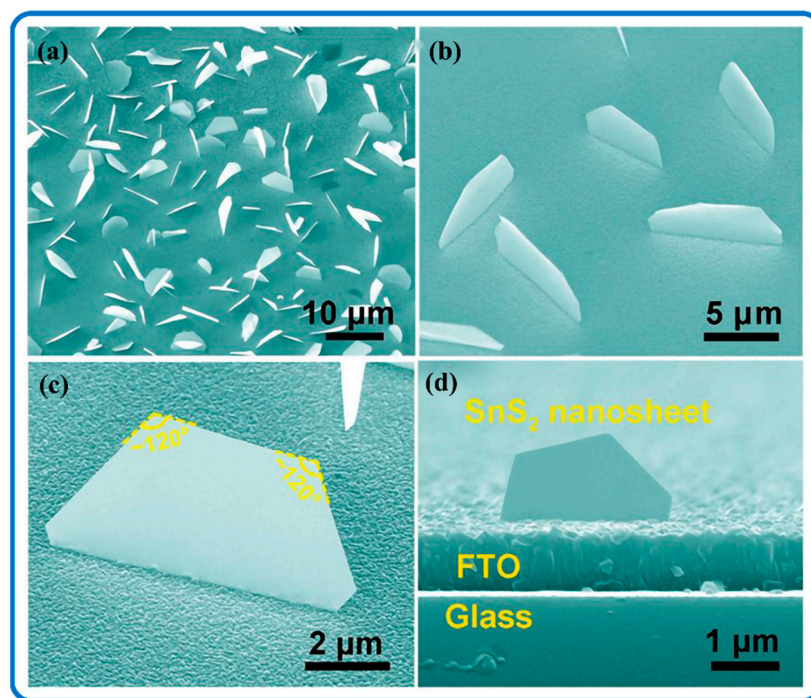


Figure 6. (a,b) Low-magnification SEM images. (c) High-magnification SEM image of vertical SnS₂ nanosheet taken at 45° from a normal viewing angle. (d) Typical cross-sectional-view SEM image of one vertical SnS₂ nanosheet grown on FTO substrate. Reproduced with permission from [126]. Copyright 2017, Royal Society of Chemistry.

3.1.4. Three-Dimensional (3D) Self-Supporting SnS₂ Nanoflowers

Three-dimensional SnS₂ nanomaterials have hierarchical flower-like architectures with nanosized building blocks and a complex assembled architecture. Their large surface area can reduce the concentrated polarization and offer more sites for accommodation [127]. Figure 7a,b are flower-shaped nanostructures analyzed by TEM and SEM analysis. Figure 7c,d represents the TEM images of SnS₂ nanoflowers and the fringe interval with the d-spacing of hexagonal SnS₂, respectively. The schematic approach leading to the formation of SnS₂ nanoflowers is demonstrated in Figure 7e [128,129]. Xiong et al. also described well-defined SnS₂ nanoflowers for NH₃ detection by a facile solvothermal method [130]. On the other hand, 3D hierarchical SnS₂ microspheres consisting of thin-layered nanosheets were synthesized via a one-pot hydrothermal method [131]. By altering

the ratio of SnCl_4 to L-cysteine, they were able to keep their morphologies under control. In addition, mild hydrothermal treatment in the presence of octyl-phenol-ethoxylate (Triton X-100) at 160°C led to the achievements of 3D nanoflowers with a spot-like appearance along the $[010]$ axis of the SnS_2 crystal [132].

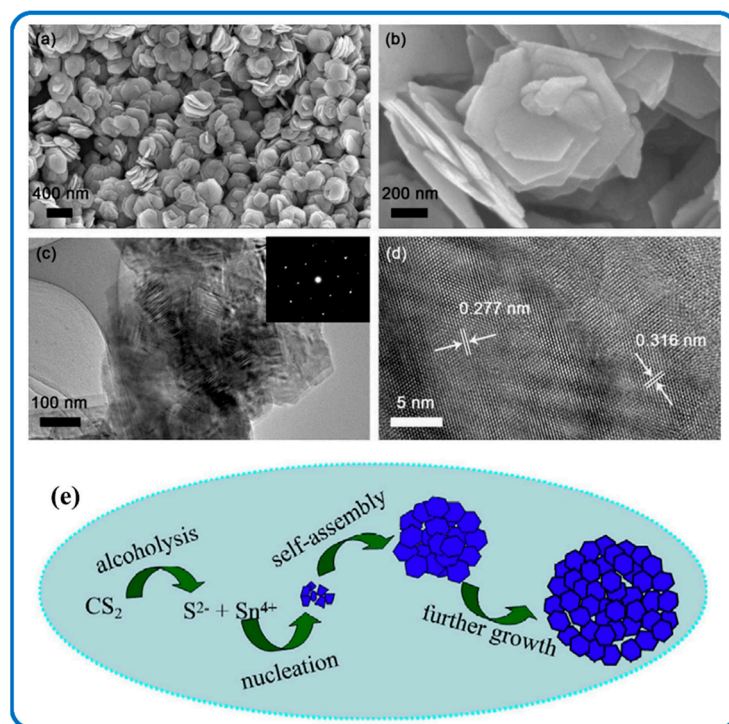


Figure 7. (a,b) SEM, (c) TEM images, and (d) Fringe interval of the as-prepared SnS_2 nanoflowers. Reproduced with permission from [128]. Copyright 2018, Elsevier. (e) Schematic illustration of 3D SnS_2 nanoflowers. Reproduced with permission from [129]. Copyright 2013, Elsevier.

3.2. Dimensional Characteristics of SnS_2 /Carbon Composite Nanomaterials

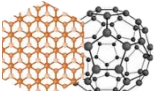
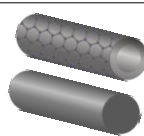
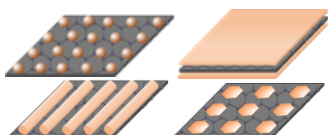
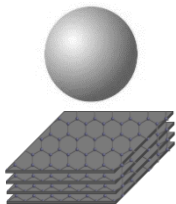
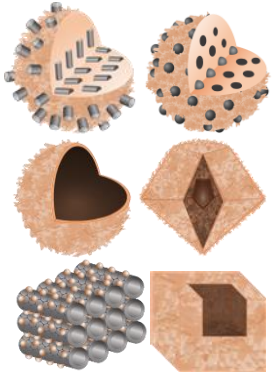
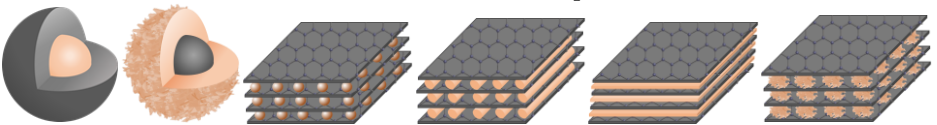
The hybrid structures of SnS_2 /Carbon materials at the nano level have permitted the control of desired properties and features. Table 2 suggests the possible hierarchical formation of SnS_2 /Carbon composite nanomaterials. It tries to depict the synergies between SnS_2 nanostructures and carbon nanomaterials in the hybridized structures. The concept of composites further tries to enhance the nanomaterials' internal and external capabilities as well as the physical/chemical compatibility. The unique properties of these composite nanomaterials are of great interest for their environmental and energy storage applications.

3.2.1. Zero-Dimensional (0D) SnS_2 /Carbon Composite Nanodots

Various questions come up about what constitutes 0D hybrid materials. The literature captures this concept of zero-dimensional composites giving preference to one component. The individual nanostructures of SnS_2 and carbon have achieved great heights in many applications, for example, in the fields of photoelectric detectors, solar photocatalysts, and photovoltaic solar cell applications. To the best of our knowledge, there are no reports on zero-dimensional composite SnS_2 /Carbon nanomaterials. SnS_2 /Carbon nanostructures could result from a combination of SnS_2 QDs and Carbon QDs in a hybridized synthesis approach. The achievement of this structural material at a low dimension has proven beneficial in its application in catalysis and electrochemistry [133]. Chen et al. found that the tiny size of SnS_2 QDs makes them easy to insert into graphene nanosheets which prevents the restacking of graphene nanosheets [134]. Meanwhile, the inserted SnS_2 QDs showed an enhanced photocatalytic effect. The carbon dots- SnS_2 nanomaterials could show excellent photocatalytic adsorption capacity by acting as a good electron acceptor.

Therefore, a synergetic combination of SnS₂ QDs and carbon QDs could be a powerhouse for future applications.

Table 2. Schematic comparison of different hybrid nanostructures of SnS₂/Carbon composite nanomaterials.

Dimension	SnS ₂ Structures	Carbon Structures	Published Composite Nanomaterials	Ref.
0D				[91]
1D				[58,92,95,135–138]
2D				[89,139–143]
3D				[111,136,144–150]
Potential structures of SnS ₂ /Carbon composite nanomaterials				
				

The schematic images in Table 2 were adapted with permissions from [58], copyright 2011, American Chemical Society; [92], copyright 2018, Elsevier; [135], copyright 2014, Royal Society of Chemistry; [136] copyright 2018, Elsevier; [138], copyright 2016, Royal Society of Chemistry; [89], copyright 2017, Elsevier; [139], copyright 2019, Zhang et al. (CC BY); [140], copyright 2019, American Chemical Society; [141], copyright 2020, American Chemical Society; [142], copyright, 2017, American Chemical Society; [143], copyright 2011, Royal Society of Chemistry; [111], copyright 2017, Elsevier; [144], copyright, 2020 Wiley-VCH; [145], copyright 2021, Elsevier; [146], copyright 2021, Elsevier; [148], copyright 2015, Elsevier; [149], copyright 2019, (CC BY 4.0), [150], copyright 2021, (CC BY-NC-ND 4.0).

3.2.2. One-Dimensional (1D) SnS₂/Carbon Composite Nanomaterials

Controlling the orientation and polymer chain alignment of 1D nanostructures can increase their multifunctional features such as thermal and electrical conductivity [151]. The characteristic properties of hierarchical 1D composite nanomaterials are usually realized by using one of the components as a backbone or template material, and the other component is deposited on the surface or within it [152–154]. An understanding of 1D nanostructures has been intensively covered by Wei et al. [155], where the fabrications and applications of 1D mono and hybrid nanomaterials are touched on. In most 1D SnS₂/Carbon hybrid

formations, the SnS₂ part, usually nanosheets or nanoflakes is embedded in the 1D carbon template parallelly or inclined at an angle. This enhances the properties of SnS₂/Carbon nanomaterials and correspondingly influences their applications [138]. SnS₂/CNT composite nanomaterials are gaining attention because of their large surface area and the improved conductivity compared to SnS₂. The sheet size of SnS₂ is greatly reduced when it is clustered in SnS₂/CNT hybrid nanocomposites, indicating that the introduction of CNTs refined the sheet size of SnS₂ [156]. This leads to the CNTs evenly wrapped on the surface of or interspersed in the SnS₂ sheets which is beneficial for improving the conductivity of the SnS₂. In addition, SnS₂/CNTs can be attached to the surface of the separators without any peeling and blanking, thus showing good flexibility and mechanical stability [94,157]. In an extraordinary case, the CNTs could act as templates for SnS₂ materials. Jin et al. demonstrated this by filling hard CNT templates with Sn materials and sulfurizing beyond 300 °C to achieve SnS₂ nanostructures as a dominant phase within the CNTs [97]. Again, the diffraction peak corresponding to the (001) plane of SnS₂/CNT hybrid nanostructures exhibits preferentially oriented growth along this plane. Figure 8 demonstrates a typical formation of 1D SnS₂/Carbon composite nanostructure through a facile templating synthesis using MnO_x nanorods as templates [136]. By adjusting the sulfurization temperature, it aided in the structural control during the formation of the nanocomposite, such that the SnS₂ nanosheets were encapsulated in amorphous carbon nanotubes.

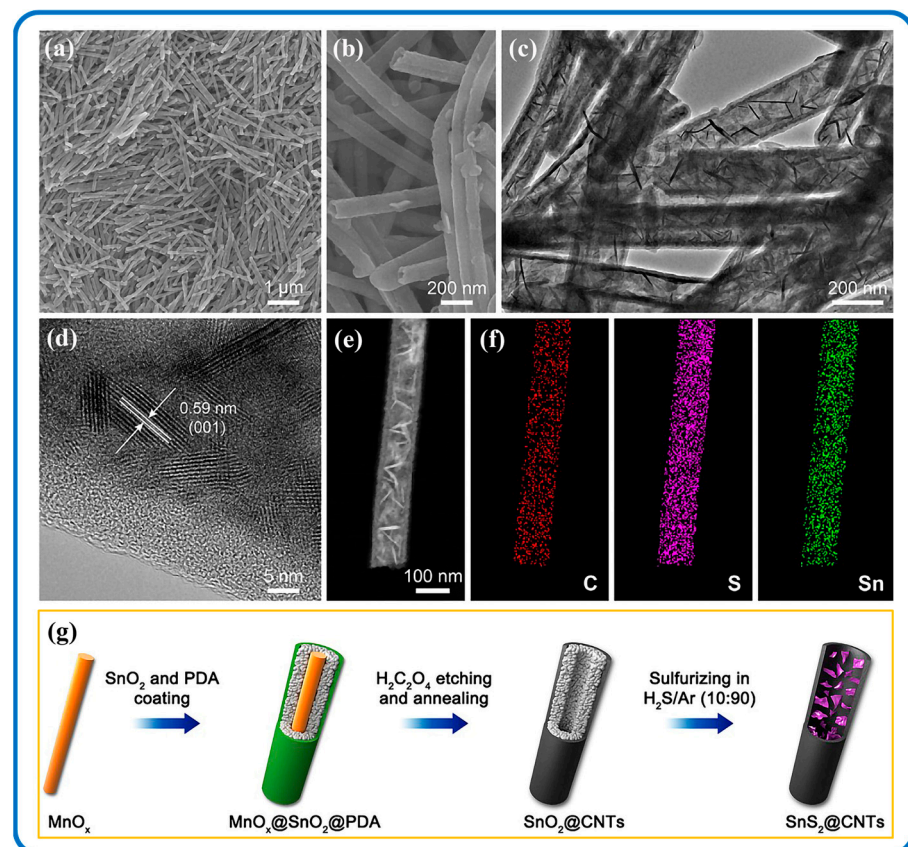


Figure 8. (Characterization of SnS₂@CNTs in terms of morphology and structure, (a,b) FE-SEM images, (c) TEM image, (d) HRTEM image showing SnS₂ nanosheet with evident lattice fringe space of 0.59 nm, (e) High-angle annular dark-field scanning transmission electron microscope (HAADF-STEM) image of one individual SnS₂@C nanotube, and (f) elemental mapping of SnS₂@C nanotube, corresponding to C, S, and Sn elements. (g) Synthesis of SnS₂@CNTs depicted schematically. Reproduced with permission from [136]. Copyright 2018, Elsevier.

The carbon nanofiber network has also made feasible contributions in terms of SnS₂/Carbon nanomaterial formation. For instance, Xia et al. prepared SnS₂ embedded in

nitrogen and sulfur dual-doped carbon (SnS_2/NSDC) nanofibers by a facile electrospinning technique as indicated in Figure 9 [92]. Figure 9d–f illustrates the various morphological features of the $\text{SnS}_2/\text{Carbon}$ composite nanofibers. The carbon nanofiber framework provides a conductive host and is tolerant to the volume variation of SnS_2 during the charging/discharging processes, thereby maintaining the structural stability of the $\text{SnS}_2/\text{Carbon}$ electrode [158]. Furthermore, the microstructures of SnS_2 nanosheets can provide rich migration paths of sodium ions and electrons; therefore, the hybridized synergy realizes a rapid and efficient electron transport, which leads to an enhanced performance of the $\text{SnS}_2/\text{Carbon}$ system [159–162].

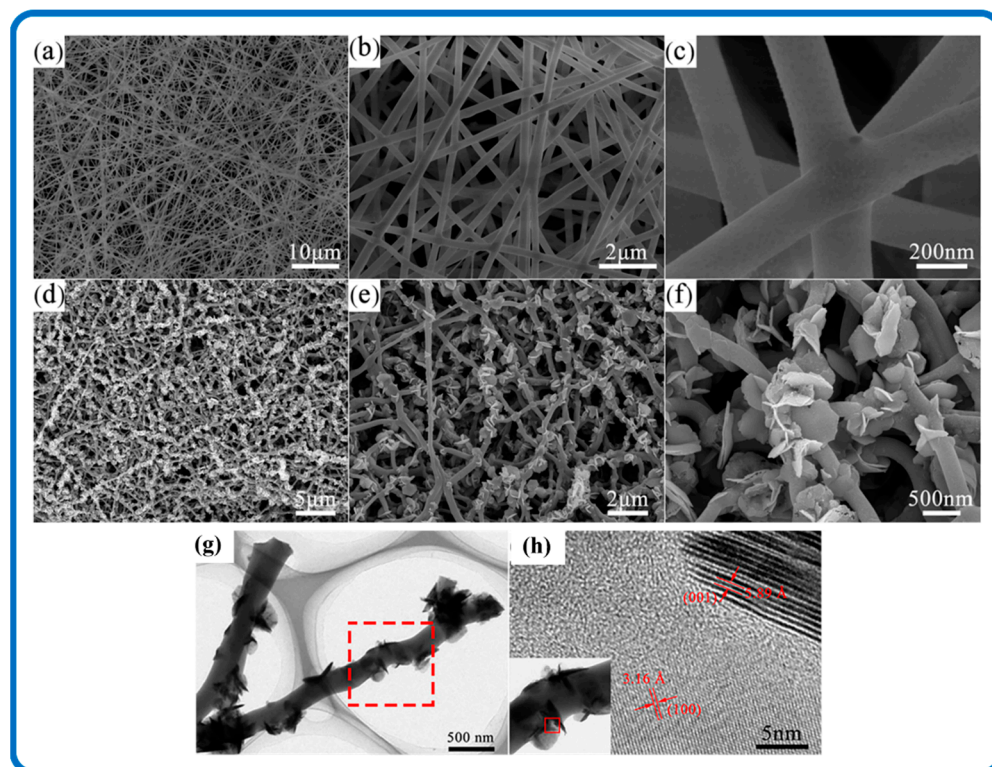


Figure 9. (a–c) Different-magnification FE-SEM images of carbon nanofibers and (d–f) SnS_2/NSDC nanofibers. (g) TEM image of SnS_2/NSDC nanofibers. (h) HRTEM image of SnS_2/NSDC nanofibers marked in the red area. Reproduced with permission from [92]. Copyright 2018, Elsevier.

3.2.3. Two-Dimensional (2D) $\text{SnS}_2/\text{Carbon}$ Composite Nanomaterials

The sheet-like nature of 2D nanomaterials makes them attractive for resolving diverse application demands. Coupled with SnS_2 , 2D $\text{SnS}_2/\text{carbon}$ nanomaterials display a wide range of extraordinary properties especially in alleviating volume expansion [163]. Especially, minimal stacking of 2D layered materials can be achieved for better application performance due to the introduction of the conductive graphene layers, which conveniently protects the SnS_2 nanosheets from breakdown and weakens their agglomerating and restacking trends. Through an all-solid-state synthesis approach, Lonkar et al. achieved the minimal stacking of SnS_2 nanosheets and realized a scalable 2D SnS_2 and graphene layered nanosheets (SnS_2/G) via ball milling using robust mixed precursors and sufficient metal-sulfur intercalation within the GO substrate [141]. Furthermore, it showed great inherent conductivity, high specific surface area, and high catalytically active planes, which is a plus in battery applications.

Two-dimensional nanostructures are considered as architectural building blocks to hasten reaction kinetics and shorten the transport paths of electrons and ions. Therefore, the 2D synergistic combination of SnS_2 with 2D carbon materials would be vital in enhancing its application. For example, SnS_2 itself experiences low catalytic and electrical activity,

but the existence of strong interfaces between SnS₂ and graphene might facilitate and ease charge transportation [164]. Furthermore, the carbon component serves as a bridge for SnS₂ nanomaterials which serves as a transfer highway to improve the efficiency of charge transportation. This has proven to be beneficial in improving the overall charge transportation of the resulting nanocomposites. Figure 10 shows fabricated 2D SnS₂ nanoplates anchored on rGO nanosheets by a one-step controllable hydrothermal synthesis approach followed by a slight reduction reaction [165]. The face-to-face (FTF) nanostructure allowed for a large contact area, which improved the composite's conductivity and reduced the migration distance of Na⁺ and electrons between rGO and SnS₂.

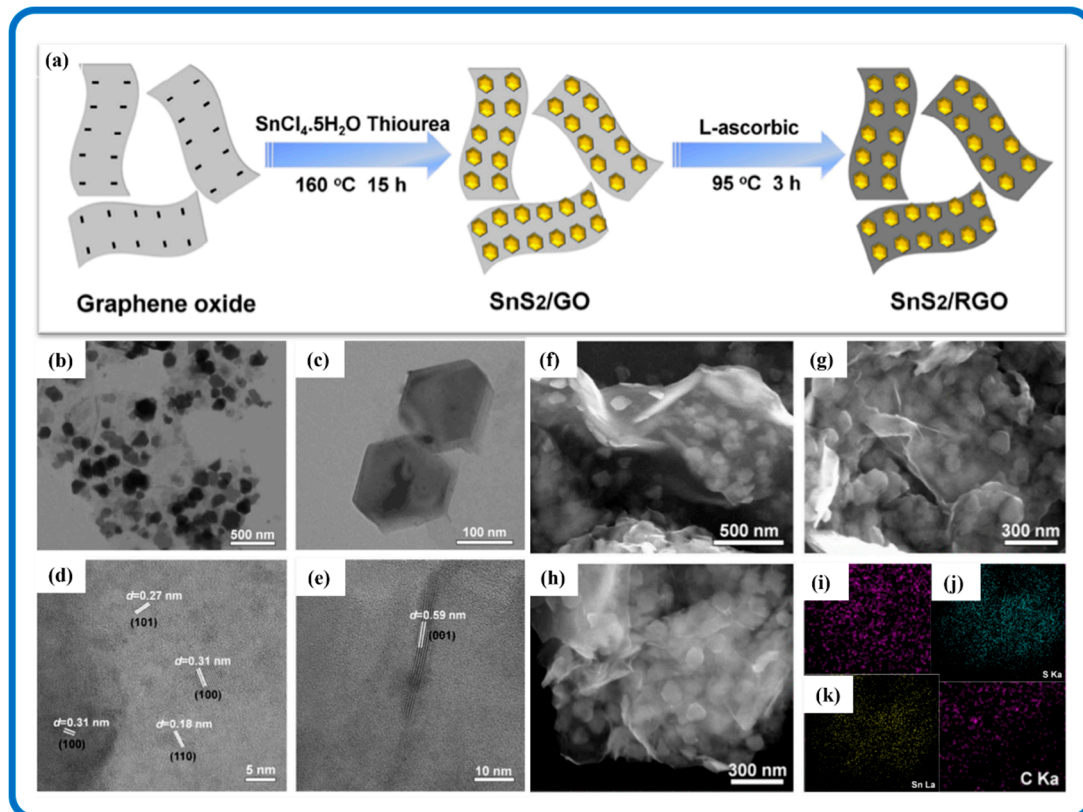


Figure 10. (a) Schematic illustration of the fabrication process for the SnS₂/rGO composite, (b,c) TEM and (d,e) HRTEM images of the SnS₂/rGO composite, (f–h) SEM images of the SnS₂/rGO composite, and (i–k) the elemental mapping of C, S, and Sn, respectively, corresponding to (h). Adapted with permission from [165]. Copyright 2017, Elsevier.

In addition, the charge transfer resistance tests of 2D nanocomposites demonstrated superior transportation kinetics as shown in Figure 11, which may originate from the fast electron transport of FTF SnS₂/Carbon composites [104]. These features have also been seen in photocatalytic SnS₂/Graphene hybrid nanosheets with identically 2D structural configurations where SnS₂ nanoplates were evenly distributed across the graphene framework [166]. Wang et al. used mixed processes of hydrothermal and vapor-phase polymerization to successfully produce triaxial nanocables of conducting polypyrrole@SnS₂@carbon nanofiber (PPy@SnS₂@CNF) [93]. The nanostructures showed a porous and interconnected nanofiber network with outstanding battery application.

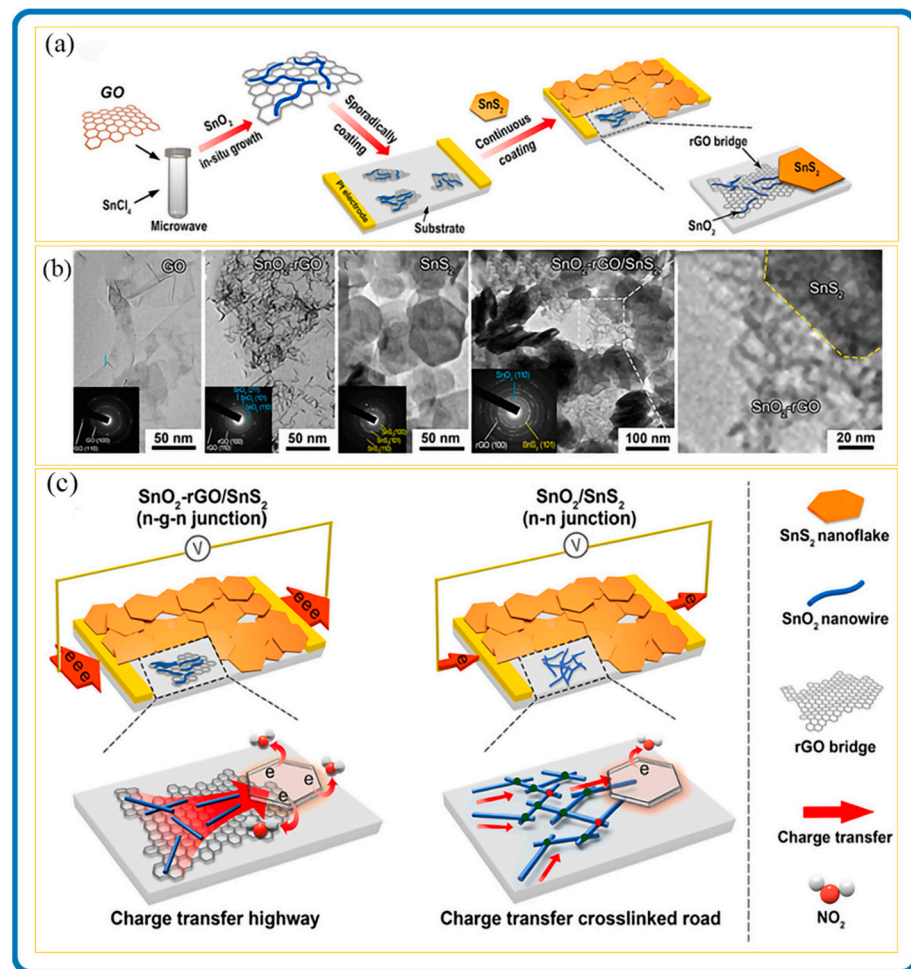


Figure 11. (a) Schematic diagram of the construction of ternary SnO₂-rGO/SnS₂ gas sensor with n-g-n junctions. (b) Subsequent TEM images. (c) Schematic images of charge transfer modification between SnO₂-rGO/SnS₂ sensor with novel n-g-n heterojunctions and SnO₂/SnS₂ sensor with traditional n-n junctions. Reproduced with permission from [104]. Copyright 2021, Elsevier.

3.2.4. Three-Dimensional (3D) Self-Supporting SnS₂/Carbon Nanomaterials

Three-dimensional nanostructures of SnS₂/Carbon nanomaterials are usually not confined to the nanoscale in any dimension. Three-dimensional nanostructures offer appreciable expanded levels of functionality compared to 2D counterparts because the strains of the 3D shape can induce bending and twisting below the maximum endurance limit for each layer in the construct [167]. Three-dimensional SnS₂/Carbon composite nanostructures could result from different synthesis approaches with different combinations of SnS₂ and carbon precursors. In general, 0D, 1D, and 2D nanomaterials are the building blocks to achieving desired structural nanocomposites. The dispersions of the nanomaterials could include, for example, nanodots, nanotubes, or nanosheets as well as multi-nano layers. These structural elements are usually in close contact with each other, thereby resulting in 3D interfaces. Many 3D nanocomposite combinations have been reported in the literature [168–170]. For example, through the hydrothermal synthesis method, carbon nanotubes formed a cross-winding network on the surface of SnS₂ nanoplates. This resulted in flower-like SnS₂/Carbon composite nanostructures via electrostatic interactions as shown in Figure 12a–d [111]. The diameter of the CNTs was 25 nm with a length of 1–3 μm (Figure 12d). The hybridized 3D SnS₂/Carbon structures could alleviate the internal stress induced by the volumetric expansion/contraction during Li⁺ insertion/extraction processes [148]. Liu et al. obtained uniform 3D interpenetrating porous membrane nanostructures of SnS₂/Carbon fabricated via non-solvent-induced phase separation (NIPS)

membrane technology, and this technology offered an abundant membrane pore space for uniform SnS₂ nanosheet development via C–S covalent bonding [171].

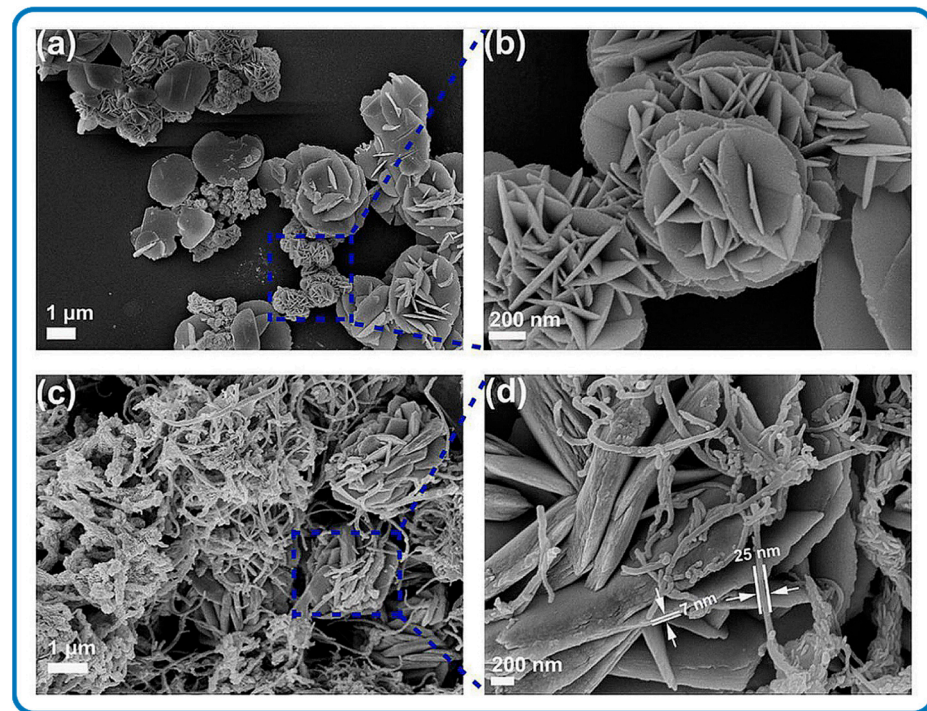


Figure 12. SEM images of (a,b) SnS₂ and (c,d) SnS₂/CNTs. Reproduced with permission from [111]. Copyright 2016, Elsevier.

Aside from 3D network composite nanomaterials, hollow 3D composite nanostructures are quite common and have shown unique properties in energy storage fields. Li et al. reported hollow 3D SnS₂/Carbon nanospheres that were designed through a facile solvothermal route followed by an annealing treatment (Figure 13a). The SnS₂/Carbon nanocomposite resulted from using SnO₂@C hollow nanospheres as a template and thioacetamide as a sulfur source as shown in Figure 13c. Moreover, the hollow structure and morphology were maintained during the synthesis process. The 3D SnS₂/Carbon nanospheres showed substantial structural integrity reinforcement during electrochemical reactions with improved sodium storage properties. Furthermore, there was high reversible capacity due to a large number of active sites, ideal void space and porosity for volume expansion, high surface permeability, and favorable kinetics due to the high face-to-volume ratio of the hollow structure.

Nowadays, 3D composites of SnS₂/Carbon architectures are becoming an academic hotspot with optimal rate capability and cycling stability owing to the synergism of active SnS₂ particles and an extremely conductive carbon framework. Three-dimensional carbon fiber and graphene foam have served as a conductive and robust skeleton for SnS₂, and their TEM imaging demonstrated that the SnS₂ nanoflakes were strongly attached to these materials [172,173]. The graphene-assembled architectures can adapt hierarchical morphology with high surface-area-to-volume ratios and construct macroscopic and large-size monolithic materials, indicating that they have considerable technological promise for a variety of sustainable applications [174].

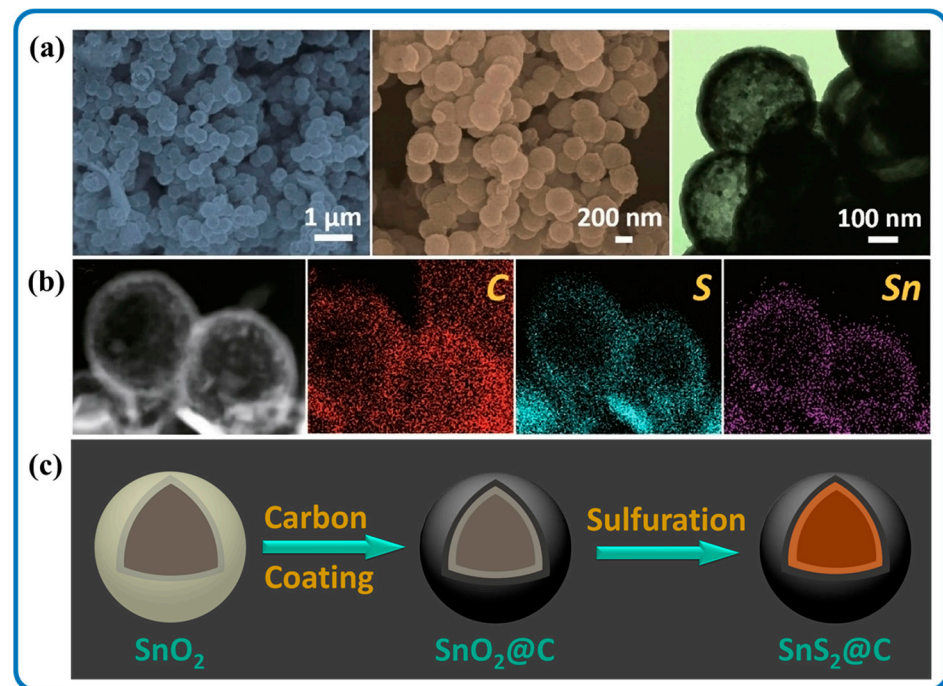


Figure 13. (a) TEM images of composite SnS₂/C, (b) elemental mapping images of C, S, and Sn, (c) Schematic illustration of SnS₂/carbon nanocomposite fabricated from SnO₂. Reproduced from [112]. Copyright 2019, Springer, Open Access.

4. Applications of Synthesized SnS₂ and SnS₂/Carbon Nanomaterials in Environmental Remediation, Electrochemical Energy Conversion, and Storage

Due to its extensive availability, biocompatibility, cheap cost, low toxicity, and high chemical stability, SnS₂ is one of the most economically viable materials exploited in a wide range of applications. In addition, SnS₂ possesses good qualities such as a high surface area with increased active sites, good ion exchange capability, and loading capacity. The hybridization of SnS₂ with carbon materials has been explored in catalysis, biomedicine, supercapacitors, electrochemical sensors, batteries, photocatalysis, and so on. In particular, their capacity to build dimensionally variable structures gives SnS₂ and SnS₂/Carbon nanomaterials significant structural advantages in environmental remediation and electrochemical energy conversion and storage. The applications of SnS₂ and SnS₂/Carbon nanomaterials have been briefly summarized in Figure 14.

4.1. Photocatalyst in Pollutant Degradation

Photocatalysis has shown great potential in hydrogen production, antibacterial activity, pollutant degradation, air purification, etc. [175–179]. Amongst them, photocatalytic pollutant degradation is a particularly appealing technology since organic pollutants can be entirely degraded into CO₂, H₂O, and inorganic compounds leaving minimum detrimental leftovers [180,181]. For decades, semiconductor-based photocatalysts such as SnO₂, ZnO, TiO₂, etc., have gained prominence as breakthrough material for organic pollutant degradation [182]. This is due to their ability to use solar energy to carry out the catalytic reaction [183]. Amongst them, TiO₂ has gained wider recognition due to its abundance and low cost. However, drawbacks of TiO₂ such as a wide bandgap (3.2 eV), limited active sites, low absorption of UV light, and low quantum efficiency impede its versatility in the efficient degradation of pollutants [184]. Therefore, it is imperative to design a unique photocatalyst with high absorption capacity and a narrow bandgap for photocatalysis. SnS₂ and its hybrid nanocomposites are gaining massive recognition in the scientific community as alternative photocatalytic materials to TiO₂ as a result of their narrow bandgap and high

quantum yield [185–188]. SnS₂ composite nanomaterials have also shown higher catalytic performance than SnS₂ nanomaterials themselves in pollutant removal.



Figure 14. Applications of SnS₂ and SnS₂/Carbon nanomaterials in environmental remediation, electrochemical energy conversion, and storage.

4.1.1. SnS₂ Nanomaterials in Photocatalysis

SnS₂ nanoparticles are known to exhibit photocatalytic properties under visible light [189–191]. As a semiconductor metal sulfide, SnS₂ can act as capable sensitizers and harvest visible light for narrow bandgap semiconductors in some photocatalytic applications. Srinivas et al. found the bandgap of SnS₂ nanostructures is around 2.50 eV as the photocatalyst of the irradiation of visible light [192]. SnS₂ QDs have shown a bandgap that matches the absorption spectra of sunlight, a huge extinction coefficient due to quantum confinement, and large intrinsic dipole moments. However, the reduction in particle size has shown an increase in the bandgap of the semiconductor nanomaterials [193]. Nonetheless, various dimensions of SnS₂ nanomaterials have reported successes in photocatalytic activities. For example, 1D SnS₂ nanotubes have demonstrated big potential in photocatalysis with more active sites for adsorption and catalysis [194]. These properties have also been exhibited by 2D SnS₂ nanomaterials [77,195]. For instance, atomically ultrathin 2D SnS₂ conducting channels helped to achieve rapid carrier transport in photoelectrodes which greatly reduced the recombination rate with a bandgap of 2.29 eV [196]. Moreover, the lower thickness of 2D SnS₂ structures provided an easy pathway for photogenerated electrons and holes to move toward the surface reaction sites [195]. Hence, the possibility of recombination is reduced, and photocatalytic effectiveness is improved. Ullah et al. in a comparative study observed that SnS₂ and conventional cadmium sulfide (CdS) films have direct bandgap values of 2.20 eV and 2.45 eV, respectively [197].

Moreover, it was discovered that SnS₂ film has a higher photocurrent of 140 μ A than CdS films with 80 μ A. Thus, compared with CdS, SnS₂ nanostructures offer a better bandgap, superior cycling stability, and bigger reversible capacities that are desirable for photocatalysis and electrocatalytic applications. Three-dimensional SnS₂ nanoflowers prepared at 120 °C in solvent ethylene glycol have been proven to have high adsorption capability and visible light photocatalytic activity for dyes (Methyl Blue and Methyl Orange) and heavy metal ions (Pb²⁺ and Cd²⁺) [198]. Microwave-assisted synthesis of hexagonal SnS₂ allowed for the simultaneous adjustment of morphologies and nanostructures under

atmospheric pressure and low temperature [199]. Moreover, it showed advantages in the photoreduction of stable azo-dye. In addition, SnS₂ nanostructures showed excellent photocatalytic activity in the reduction of hazardous Cr(VI) to harmless Cr(III) in environmental conditions, as well as effectively decomposing mutagenic dyes (Methyl Orange and Rhodamine Blue) to benign compounds in a brief duration [192].

It is apparent that all dimensional SnS₂ nanomaterials can be harnessed for photocatalytic applications due to their semiconductor nature. Researchers are drawn to this exceptional catalytic feat because it allows them to include and synthesize composite nanostructures with improved performance. Moreover, the bandgap is an important parameter in photocatalytic activities. Besides adsorption capacities, semiconductor catalysts with a narrow bandgap can absorb more photons, resulting in better catalytic activity when exposed to visible light [200]. New modifications are being used during synthesis to further optimize the bandgap for visible light application. One such modification is the introduction of carbon precursors to achieve SnS₂/Carbon composite nanomaterials with desired morphological orientations and photocatalytic properties.

4.1.2. SnS₂/Carbon Nanomaterials in Photocatalysis

Carbon materials can form unique chemical bonding thus providing strong interactions with SnS₂, which leads to a bandgap narrowing effect [201]. SnS₂/Carbon composite nanomaterials show more active sites, electron acceptors, and transport channels with improved structural stability and adsorption ability [202]. SnS₂/Carbon nanomaterials have been reported to have the ability to degrade organic pollutants and carcinogens more effectively as compared to SnS₂ (i.e., CO₂) [103,203]. Xue et al. in their research used heterojunction bio-carbon/SnS₂ nanocomposites with a narrow bandgap to efficiently photocatalyze the conversion of Arsenic(III) and calcium arsenate removal [204]. The -C=Sn-S bonds efficiently prevented SnS₂ agglomeration, extended the photoresponse range, and enhanced the hydrophilicity of the bio-carbon/SnS₂ nanocomposites while reducing their transfer resistance. For example, Figure 15 shows the sheet-like SnS₂ nanoparticles uniformly incorporated on rGO sheets. Because of the increase in interfacial charge carriers, the addition of rGO to the composite nanomaterials improved the photocatalytic activity of Cr (VI) reduction. The SnS₂/rGO composite photocatalysts also outperformed pure SnS₂ QDs in terms of photocatalysis. So, the synergy between SnS₂ and carbon materials at the nanoscale can provide a sufficient bandgap to catalyze photocatalytic reactions. A substantial bandgap is necessary to significantly promote the photocatalytic abilities of SnS₂/Carbon composite nanomaterials [205].

The recombination inhibition of charge carriers between SnS₂ and the carbon materials has been observed to bring about the optimization of charge carriers at the SnS₂/carbon interfaces to photodegrade Cr(VI) [207]. This was achieved through the coupling effect and the strong electrostatic attraction of carbon materials, which served as the electron acceptor to trap the photoinduced electrons from SnS₂ and thus enhances the separation efficiency of electrons and holes [208]. However, the degradation of toxic substances is further impacted by the concentration of the pollutants and the dosage of the catalysts. Figure 16 further shows a schematic illustration of the mechanism in the photocatalytic breakdown of organic and inorganic pollutants by SnS₂/Carbon composite nanomaterials. As shown in the diagram, once illuminated by light, electrons get excited and then migrate from the valence band (VB) to the conductor band (CB) of SnS₂ QDs. Subsequently, the SnS₂ electrons transfer to the associated carbon nanostructures that act as electron acceptors. This suppresses the recombination of photogenerated electron-hole pairs leading to ·OH and ·O²⁻ radical species, which can lead to the removal of pollutants by their superior activities.

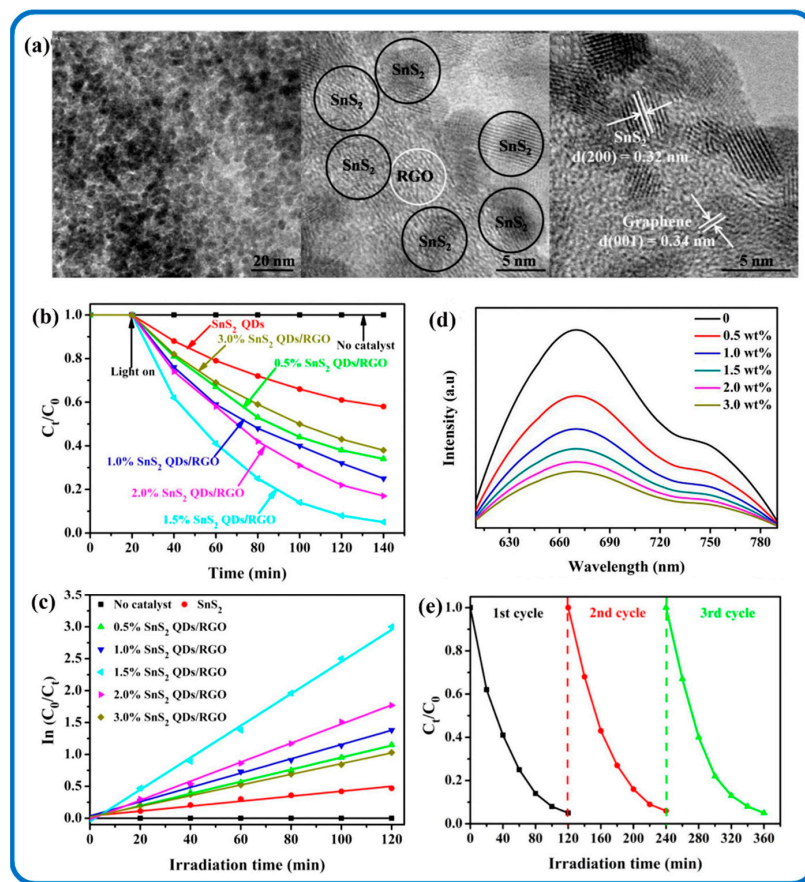


Figure 15. SnS₂ QDs/rGO nanocomposite photocatalyst (a) TEM and HRTEM images, (b) Cr (VI) reduction efficiency by photocatalysis, (c) kinetic linear simulation curves of Cr(VI) degradation, (d) UV-vis absorption spectra of SnS₂ loaded with different amounts of rGO, and (e) cycling runs of the photoreduction of Cr(VI) in the presence of SnS₂ QDs/rGO photocatalyst. Adapted with permission from [206]. Copyright 2016, Elsevier.

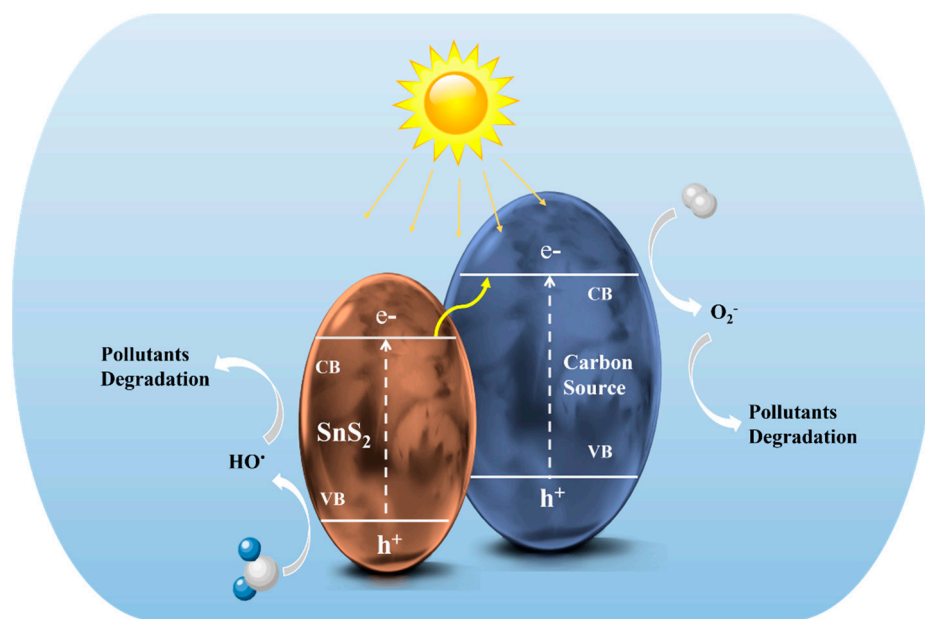


Figure 16. Photocatalytic schematic representation of SnS₂/Carbon nanomaterials.

Table 3 shows the comparative photocatalytic performances of SnS₂ and SnS₂/Carbon composite nanomaterials under visible light from various literature. It can be observed that the synergistic combination of SnS₂ nanomaterials and the carbon allotropes significantly enhanced the photocatalytic efficiency of the SnS₂/Carbon composite nanomaterials compared with SnS₂. Notably, dimensional SnS₂/Carbon nanomaterials exhibited remarkable degrading effects especially on chromium (VI). Overall, SnS₂/Carbon nanomaterials hold great degradation potential toward wastewater treatments. Photocatalysts are usually made of costly precious metals that are not in abundance. With the availability and low cost of SnS₂ and carbon materials, researchers can venture more into creating SnS₂/Carbon photocatalytic nanomaterials to harness its potential in photocatalysis at a large scale.

Table 3. Comparison of the photocatalytic activity of SnS₂ and SnS₂/Carbon nanomaterials on pollutant remediation.

Dimension	Photocatalysts	Pollutants	Photocatalytic Efficiency (%)	Irradiation Time (min)	Ref.
0D	SnS ₂ Quantum Dots	Chromium (VI)	92	120	[118]
	SnS ₂ Nanoparticles	Methyl Orange	90	60	[199]
	SnS ₂ QDs/rGO	Chromium (VI)	95.3	120	[206]
	SnS ₂ QDs/N-doped Graphene	Methyl Orange	95.6	60	[134]
1D	SnS ₂ Nanotubes	Chromium (VI)	53.0	60	[194]
	CNT@MoS ₂ /SnS ₂	Chromium (VI)	~100	90	[202]
2D	SnS ₂ Nanoflakes	Rhodamine B	61	120	[44]
	SnS ₂ Nanoflakes	RR 120 Dye	-	180	[78]
	SnS ₂ Nanoplates	Methyl Blue	85	120	[195]
	SnS ₂ /rGO	Chromium (VI)	94.0	90	[60]
	Bio-carbon/SnS ₂ Nanosheets	Arsenic (III)	95.1	-	[204]
	SnS ₂ /N-Doped Carbon QDs	Chromium (VI)	100	25	[208]
	SnS ₂ -SnO ₂ /Graphene	Rhodamine Blue	97.1	60	[209]
3D	SnS ₂ Nanoflowers	Chromium (VI)	83.8	-	[27]
	SnS ₂ Nanoflowers	Methyl Orange	79.8	120	[198]
	Carbon Dot-SnS ₂	Chromium (VI)	77.3	-	[207]
	SnS ₂ /rGO	Chromium (VI)	90.0	150	[210]
	Carbon/SnS ₂	Chromium (VI)	99.7	120	[211]

4.2. Electrochemical Conversion and Energy Storage Applications of SnS₂ and SnS₂/Carbon Nanomaterials

The ever-growing demands for energy resources and environmental concerns have paved the way for the exploration and development of clean and sustainable energy alternatives. Electrochemical energy conversions and storage devices including supercapacitors, fuel cells, solar cells, and metal ions or air batteries have gained attention due to their environmentally benign nature and hold great potential as a fossil fuel replacement. Since its discovery in 2004, graphene has become one of the most promising materials in energy storage due to its remarkable electrochemical properties [212,213]. Furthermore, graphene has the tendency to form composite nanomaterials of different dimensions which helps to boost the overall catalytic and electrochemical performance. SnS₂ possesses a theoretical capacity of ~1136 mAhg⁻¹ [214] which is higher than that of graphene (744 mAh g⁻¹), [215,216] making it valuable for battery application, solely or in a composite material. SnS₂/Carbon (including various carbon allotropes) composite nanomaterials have also proven to be more efficient for energy storage systems because of their high conductivity, mechanical and thermal stability, and long cycle ability [217]. The relationship between SnS₂ and SnS₂/Carbon nanoarchitectures and their electrochemical performances are discussed below.

4.2.1. SnS₂ Nanomaterials in Electrochemical Conversion and Energy Storage

SnS₂ nanomaterials exhibit enhanced electrochemical performance due to their compact and consistent crystal structure with a reasonable thickness and crystallinity [218], which is also favorable for structural stability and quick ion transport during lithiation/delithiation processes. Various synthesis approaches are geared at improving the performance of SnS₂ nanomaterials as alternative electrode materials. However, the capacity fading of SnS₂ electrode materials persists due to significant volume changes during charging/discharging processes [219,220]. SnS₂ nanostructures with different morphologies have been fabricated to resolve these challenges.

Studies on the use of low-dimensional SnS₂ nanomaterials in electrochemical energy conversion and storage applications are scant, to the best of our knowledge. This is because SnS₂ materials can be hindered by sluggish diffusion kinetics and an unavoidable volume change during discharging and charging processes. Nonetheless, a SnS₂ nanowall electrode realized a high reversible capacity of 576 mAh g⁻¹ at 500 mA g⁻¹ and an excellent rate capability of ~370 mAh g⁻¹ at 5 A g⁻¹ in sodium ion batteries [221]. The sulfide matrix acts as a buffer to decrease the large strain caused by the volume expansion of tin nanostructures [222]. Unfortunately, in some cases, the large volume expansion induces aggregation of the Sn particles. As such, it can bring about the cracking, pulverization, and degradation of the electrode material which leads to capacity loss [223–225]. Nevertheless, flowerlike-SnS₂ nanostructures with large specific surface areas and better average pore sizes have exhibited remarkable battery performance with excellent long-term cycling stability [49,226,227]. In addition, binders with superior dispersion and cohesiveness in electrodes have shown to improve the electrochemical performance of SnS₂ as the anode for LIBs [228]. SnS₂ monolayers boost Lithium mobility, although their adsorption strength is moderate compared to other nanostructures. Rolling the monolayer into a one-dimensional nanotube increases Lithium ions' adsorption strength and diffusion rates [229].

In terms of air batteries, Khan et al. used 3D SnS₂ nanopetals as an air electrode material for hybrid Na-air batteries. It displayed a low overpotential gap of 0.52 V, high round trip efficiency of 83%, high power density of 300 mW g⁻¹, and good rechargeability of up to 40 cycles [230]. Moreover, their electrocatalytic performance was linked to oxygen reduction reaction (ORR) and oxygen evolution reaction (OER). The hybrid cell charge potential (OER) is 3.57 V at the high current density of 20 mA g⁻¹, which is comparable to the charge potential (3.47 V) of a hybrid cell with Platinum on Carbon (Pt/C), known to be the best catalyst for ORR at low current density (5 mA g⁻¹) [226]. Chia et al. explored the prospects of SnS₂ materials as alternative electrocatalysts in ORR, OER, and HER [227]. It was proven that SnS₂ has high inherent electrocatalytic activity and a fast heterogeneous electron transfer (HET) rate. Moreover, Xia et al. recently used first-principle methods based on the density functional theory to study the electrocatalytic performance of transition metal atoms supported on a SnS₂ monolayer [231]. The catalytic performance of SnS₂ for OER and ORR was shown to be significantly enhanced by the surface of the SnS₂ monolayer. There is limited literature on the use of SnS₂ solely or as a composite electrocatalyst, but gaps created in this field could be harnessed to create high-performance bifunctional ORR, OER, and HER electrocatalysts in the future.

4.2.2. SnS₂/Carbon Nanomaterials in Electrochemical Conversion and Energy Storage

Carbon nanostructures have been demonstrated to have the ability to confine active materials in composite nanostructures. The addition of heteroatoms to carbon could increase its affinity for active materials, form a strong architecture, and speed up the electron and ion transfer process [173,232,233]. When associated with SnS₂ nanostructures, SnS₂/Carbon composite nanomaterials can tolerate the volume change and enhance the ion diffusion rate through porous structure construction; thus, it is valuable in resolving the rapid battery capacity fading [234–236]. Furthermore, it can enhance the weak interaction between non-polar carbon and polar polysulfides which reduces polysulfide leakage from carbon materials in lithium-sulfur batteries (LSBs) [156,157].

SnS_2 /Carbon nanomaterials as electrode materials in LSBs are fairly recent in research but have shown to have the ability to reduce the “shuttle effect”. Zhou et al. tried to resolve the limitations in LIBs by embedding SnS_2 nanoparticles into 2D porous carbon nanosheet (PCN) interlayers to form a multi-functional (PCN- SnS_2) nanocomposite as illustrated in Figure 17 [237]. The synergy between PCN and SnS_2 nanoparticles resulted in a fast conversion of long-chain polysulfides to Li_2S . The constant conversion of polysulfides on PCN- SnS_2 to the final Li_2S product assisted in reducing polysulfide shuttle during the cycling process. The best performance was demonstrated by PCN- SnS_2 with dual physical-chemical confinement. It also improved the chemical reaction kinetics thereby diminishing the transfer of polysulfides to the lithium anode. This, in turn, reduced the “shuttle effect” during the entire charging/discharging process. Figure 17d shows a schematic illustration of the conversion process of sulfur on SnS_2 embedded in PCNs. Wei et al. in Figure 18 also created a flexible electrocatalytic membrane that could reduce polysulfide shuttling and capacity fading in LSBs with different SnS_2 /HCNF (hollow carbon nanofiber) interlayers that are 2D nanostructured. The SnS_2 /HCNF in the LSBs displayed a high-rate discharge capacity (694 mAh g^{-1} at 3C) and low-capacity fading rate (0.056% per cycle during 500 cycles at 1C). Additionally, it showed that the nanocomposite efficiently alleviated the “shuttle effect” as a result of the composite nanostructure synergy [159,238].

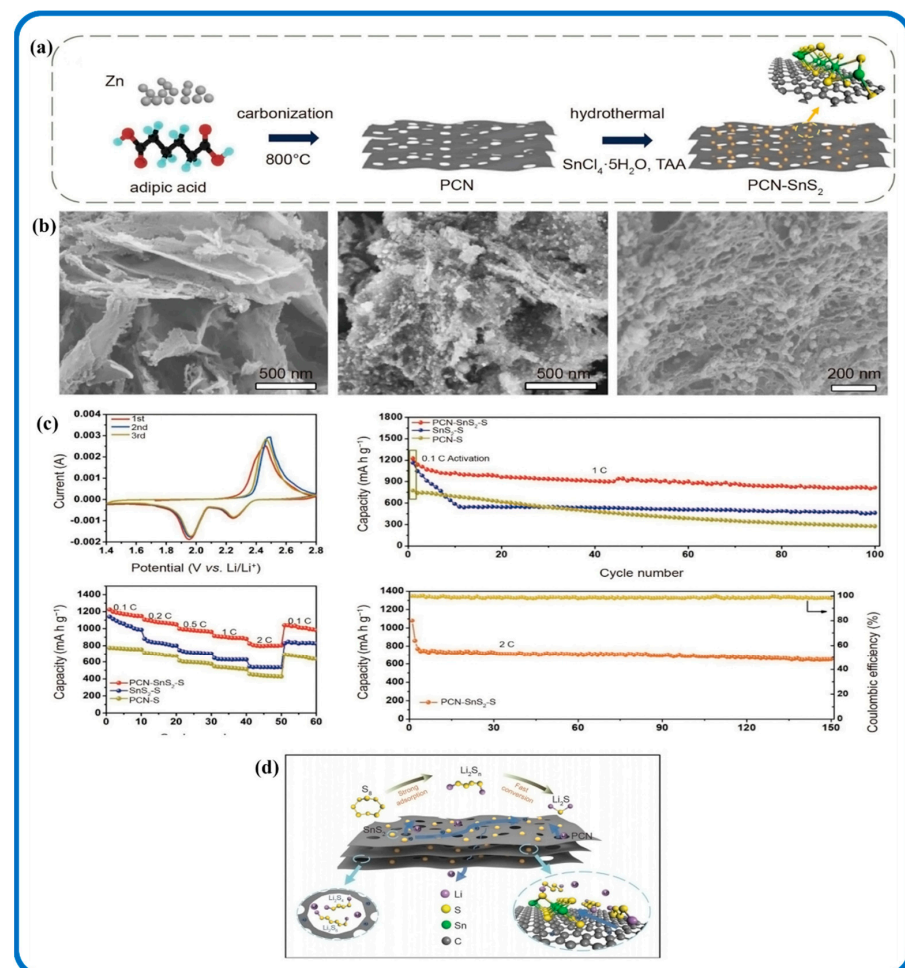


Figure 17. (a) Schematic preparation of PCN- SnS_2 composites, (b) SEM images of porous carbon nanosheets (PCN) and PCN- SnS_2 , (c) overall lithium-sulfur battery performance of PCN- SnS_2 nanocomposite, and (d) schematics of the conversion process of sulfur on PCNs- SnS_2 . Adapted with permission from Springer Nature [237]. Copyright 2021.

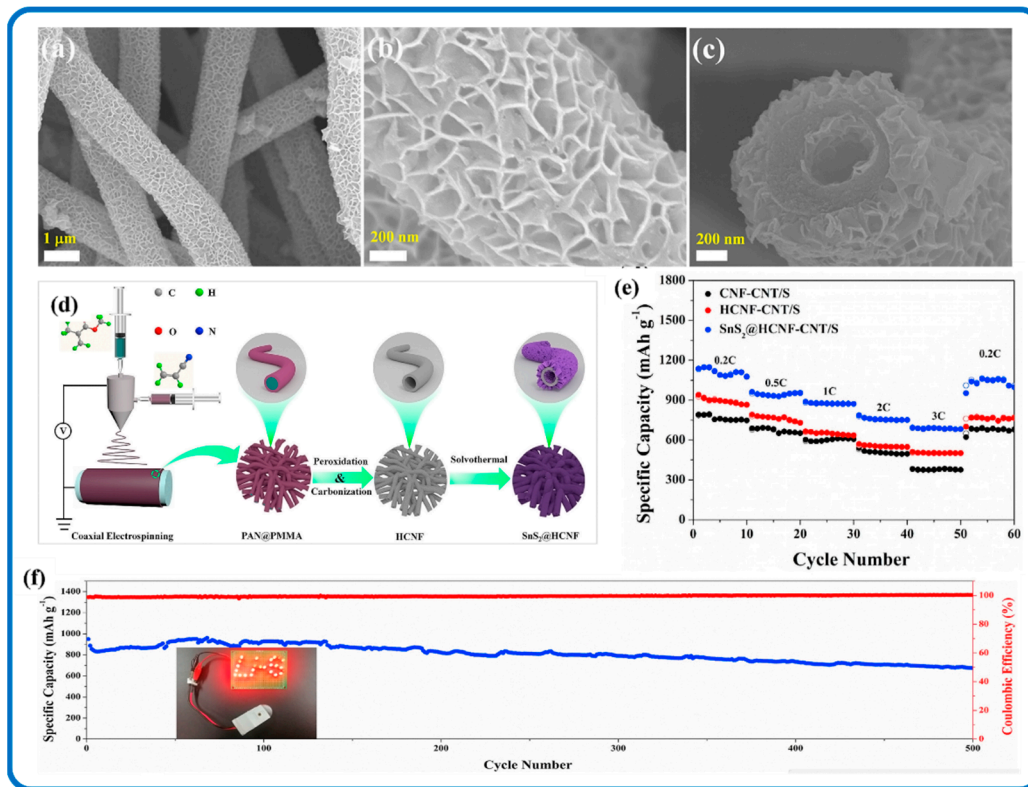


Figure 18. (a–c) SEM and TEM images, (d) schematic diagram of SnS₂@HCNF synthesis, and (e,f) electrochemical performance of Li-S batteries with different interlayers. Reproduced with permission from [239]. Copyright 2021, Elsevier.

Three-dimensional nanomaterials are the most popular dimensional SnS₂/Carbon composite nanostructures, and these nanostructures have also made an impact in energy storage applications. They have been beneficial for resolving the structure pulverization and poor electrical conductivity of metal dichalcogenides that could lead to adverse capacity decay both in LIBs and SIBs. Figure 19a,b shows the SEM image of 3D honeycomb-like rGO anchored with SnS₂ quantum dots (3D SnS₂ QDs/rGO) through spray-drying and sulfidation processes. The 3D features allowed for the volume change of SnS₂ QDs during the lithiation/delithiation and sodiation/desodiation processes. It also made provision for electrolyte reservoirs to promote the conductivity of the SnS₂ QDs. In addition, the 3D SnS₂ QDs/rGO nanocomposite electrode delivered a high capacity and long cycling stability of 862 mAh g⁻¹ for LIB at 0.1 A/g after 200 cycles (Figure 19c) and 233 mAh g⁻¹ for SIB at 0.5 A g⁻¹ after 200 cycles (Figure 19d). The improved battery performance, according to Chang et al., can be due to the composite structure's robustness and the synergistic effects among a few layers of SnS₂ and graphene [240]. Moreover, in situ-grown SnS₂ nanoparticles have been homogeneously confined in rGO and CNT porous carbon nanostructures, which resulted in 3D architectures that demonstrated outstanding performance [55].

At present, the hybridization synthesis of SnS₂/Carbon nanomaterials focuses on improving the capability and cycling stability of the electrodes [89,241]. To achieve a stable SIB/LIB electrode, Cui et al. developed self-standing electrodes with rational SnS₂ nanosheets restricted into bubble-like carbon nanoreactors anchored on N, S doped carbon nanofibers [242]. The electrodes demonstrated a very steady capacity of 964.8 and 767.6 mAh g⁻¹ at 0.2 A g⁻¹, as well as strong capacity holding of 87.4% and 82.4% after 1000 cycles at high current density, respectively. It was stated further that the addition of N, S components improved the wettability of the carbon nanofiber matrix to the electrolyte and Li ions and the electrode's overall electrical conductivity. The performances of SnS₂ and SnS₂/Carbon composite nanomaterials in battery applications are summarized in Table 4

and compared with graphene as a reference material. Numerous synthesis approaches are being harnessed to tackle these issues and formulate hybrid nanostructures with effective outcomes. This can perhaps shorten the pathway and improve the transportation speed of electrolyte ions at electrode surfaces [29].

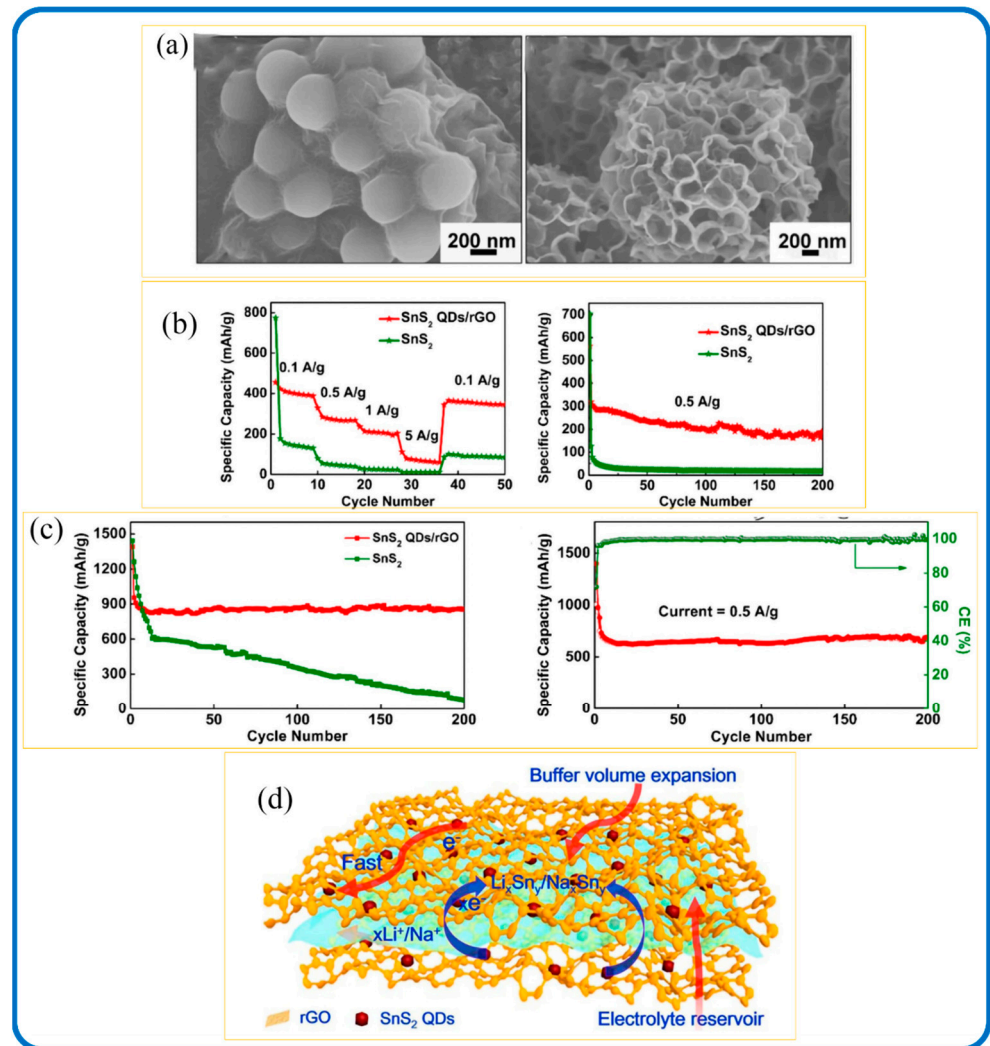


Figure 19. (a) SEM image, (b) schematic highlights during the charge/discharge processes of the 3D SnS₂ QDs/rGO composite, (c) LIBs, (d) SIB performance of the SnS₂ and 3D SnS₂ QDs/rGO composite. Adapted from [243]. Copyright 2019, Springer, Open Access.

Electrochemical reactions, such as ORR, OER, and hydrogen evolution reaction (HER) in fuel-cell and metal-air battery applications, have also shown promising successes in electrochemical energy conversion technologies [244–247]. However, research on SnS₂/Carbon composite nanostructures as electrocatalysts is rarely reported. For instance, Cheng et al. fabricated stable SnS₂ nanosheets incorporated with carbon dots, which exhibited an OER rate of up to 1.1 mmol g⁻¹ h⁻¹ under simulated sunlight irradiation [248]. Moreover, through a simple solid-state synthesis, a 2D SnS₂/Graphene nanocomposite was achieved, and it showed an electrocatalytic (HER) overpotential of 0.36 V and a specific capacitance of 565 F g⁻¹ [141]. In addition, a 3D hollow C@SnS₂/SnS nanosphere was discovered to have outstanding OER performance through structural phase transitions [145]. The Sn⁴⁺ in the composite readily received electrons in water which is vital for improving the OER activity. More so, it measured a low overpotential of 380 mV at 10 mA cm⁻² current density. Additionally, Chen et al. recently engineered SnS₂ nanosheet arrays on carbon paper with surface oxygen adjustment under the directions of density function theory (DFT)

calculations to efficiently electroreduce CO₂ into formate and syngas (CO and H₂) [249]. The SnS₂ nanosheets that were modified with surface oxygen exhibited a notable Faradaic efficiency of 91.6% for carbonaceous products at −0.9 V vs. reversible hydrogen electrode (RHE), including 83.2% for formate creation and 16.5% for syngas. These dimensional SnS₂ and SnS₂/Carbon composite nanostructures can shorten electron transfer channels in electrochemical application because of their high surface-to-volume ratio, which probably have promoted their electrochemical performance.

Table 4. Comparison of battery performances of SnS₂ and SnS₂/Carbon composite nanomaterials.

Dimension	Materials	High Reversible Capacity (mAh g ^{−1})	Cycle	Capacity Retention	Applications	Ref.
1D	SnS ₂	-	-	-	-	-
	SnS ₂ /Carbon Nanotubes	940 & 605	200	91.2% & 87.6% @100 mA/g	LIB/SIB	[55]
	SnS ₂ /Carbon Nanotubes	513.8	10	82% @100 mA/g	LIBs	[58]
	Polypyrrole/SnS ₂ /Carbon	1009	100	97.7% @100 mA/g	LIBs	[93]
	SnS ₂ /Graphene Nanorods	335	350	92% @100 mA/g	LIBs	[135]
	SnS ₂ /HCNF ¹	675	500	92.3% @ 100 mA/g	LSBs	[239]
	SnS ₂ /Carbon (MWNTs) ²	768	100	78% @ 100 mA/g	SIBs	[250]
	SnS ₂ /Carbon Nanofibers	457	~1000@2 A/g	89.5% @ 50 mA/g	PIBs ⁵	[251]
2D	SnS ₂ Nanosheets	733	50	100 mA/g	SIB	[125]
	SnS ₂ Nanoplates	521	50	90% @ 100 mA/g	LIBs	[218]
	SnS ₂ /PCN ³	816	100	-	LSBs	[237]
	SnS ₂ /EPC ⁴	443	450	89.4% @100 mA/g	SIBs	[252]
	SnS ₂ /Graphene	911	200	89% @ 100 mA/g	LIBs	[253]
	SnS ₂ /rGO	738	60	76.5% @ 0.2 C	LIBs	[254]
3D	SnS ₂ Nanoflowers	557	50	65% @ 0.1 C	LIBs	[53]
	SnS ₂ Nanoflowers	549.5	10	73% @ 100 mA/g	LIBs	[129]
	SnS ₂ Nanoflowers	502	50	84% @ 0.3 C	LIBs	[255]
	SnS ₂ /Carbon	960	300	95% @ 100 mA/g	LIBs	[256]
	SnS ₂ /Carbon-rGO	953	90	100 mA/g	LIBs	[257]
	SnS ₂ /Carbon Nanoflowers	551	50	97% @ 100 mA/g	LIBs	[148]
	SnS ₂ /Carbon Nanocubes	1080.1	200	84.1% @ 100 mA/g	LIBs	[109]
	SnS ₂ /Carbon Nanospheres	690	150 @ 1 A/g	87% @ 100 mA/g	SIBS	[110]

¹ HCNF, Hollow carbon nanofibers, ² MWNTs, Multi-walled carbon, ³ PCN, Porous carbon nanosheet, ⁴ EPC, Enteromorpha Prolifera-derived carbon, ⁵ PIBs, Potassium-ion batteries.

5. Conclusions and Perspectives

SnS₂ nanomaterials of different dimensional morphological orientations have made ample progress in photocatalysis and energy storage batteries. Meanwhile, they have presented some limitations which need further modifications to enhance their practical application potential. The broad bandgap and volume expansion during the charging/discharging processes of SnS₂ are well-known drawbacks that limit its applicability. Hybridization of SnS₂ with appropriate carbon materials, synthesizing composite nanomaterials, and developing innovative structures or morphologies dimensionally have been developed in order to overcome the aforementioned difficulties. Many novel and cost-effective synthetic methodologies have offered ways to achieve better performance in photocatalysis and energy storage batteries. SnS₂/Carbon architectural nanomaterials have become an

academic hotspot with outstanding reports on rate capability and cycling stability due to the synergism of active SnS₂ particles and a very conductive carbon framework.

Here, we have summed up some recent research on SnS₂ and SnS₂/Carbon composite nanomaterials and reviewed the progress made on the wet and solid-phase fabrication methods to achieve various morphological structures of tin disulfide (SnS₂) and SnS₂/Carbon nanomaterials such as nanodots, nanofibers, nanowires, nanotubes, nanorods, nanosheets, nanoflowers, and nanospheres in (0D–3D) dimensional states and their applications in photocatalysis, electrochemical conversion, and energy storage. We tried to bridge the knowledge gap presented in SnS₂, SnS₂/Carbon nanostructures, and their application performances in photocatalytic degradation and energy storage batteries.

Although the understanding of dimensional hybrid nanomaterials has made some achievements, there is still room to harness their dimensional capabilities, as this field of study has a lot of promise for the development of high-performance nanomaterials. In the meantime, more research into the compatibility of carbon nanomaterials with SnS₂ functional nanomaterials is needed to enhance the utilization of these hybrid nanocomposites in photocatalytic and energy storage applications. Furthermore, a deeper knowledge of the mechanisms involved in the formation of SnS₂/Carbon nanohybrids can be used to develop novel methods for producing optimal, cost-effective, and environmentally benign composite nanomaterials. Realizing these possibilities may necessitate the efforts of researchers as well as a fresh look at hierarchical nanocomposites.

Author Contributions: C.S.D.: Conceptualization, writing—original draft, revision; M.A.: Editing; Y.L.: Reviewing and editing; Y.Z.: Reviewing; Y.Y.: Conceptualization, writing—reviewing and editing, supervision, funding acquisition. All authors have read and agreed to the published version of the manuscript.

Funding: This work was supported financially by the National Key R&D Program of China (No. 2018YFE0181300), the National Natural Science Foundation of China (21905035), Liaoning Revitalization Talents Program (XLYC1907093), and the Liaoning Natural Science Foundation (20180510043).

Institutional Review Board Statement: Not applicable.

Informed Consent Statement: Not applicable.

Data Availability Statement: Not applicable.

Conflicts of Interest: The authors declare no conflict of interest.

References

1. Yuan, J.; Müller, A.H.E. One-Dimensional Organic-Inorganic Hybrid Nanomaterials. *Polymer* **2010**, *51*, 4015–4036. [[CrossRef](#)]
2. Moon, D.S.; Lee, J.K. Tunable Synthesis of Hierarchical Mesoporous Silica Nanoparticles with Radial Wrinkle Structure. *Langmuir* **2012**, *28*, 12341–12347. [[CrossRef](#)] [[PubMed](#)]
3. Cai, H.; Qiao, X.; Chen, M.; Feng, D.; Alghamdi, A.A.; Alharthi, F.A.; Pan, Y.; Zhao, Y.; Zhu, Y.; Deng, Y. Hydrothermal Synthesis of Hierarchical SnO₂ Nanomaterials for High-Efficiency Detection of Pesticide Residue. *Chin. Chem. Lett.* **2020**, *32*, 1502–1506. [[CrossRef](#)]
4. Liu, N.; Prall, B.S.; Klimov, V.I. Hybrid Gold/Silica/Nanocrystal-Quantum-Dot Superstructures: Synthesis and Analysis of Semiconductor-Metal Interactions. *J. Am. Chem. Soc.* **2006**, *128*, 15362–15363. [[CrossRef](#)]
5. Xiong, J.; Du, X.; Cheng, G.; Yang, H.; Chen, J.; Dou, S.; Li, Z. One Dimensional Hierarchical Nanostructures Composed of CdS Nanosheets/Nanoparticles and Ag Nanowires with Promoted Photocatalytic Performance. *Inorg. Chem. Front.* **2018**, *5*, 903–915. [[CrossRef](#)]
6. Mikhaylov, A.A.; Medvedev, A.G.; Grishanov, D.A.; Edison, E.; Srinivasan, M.; Sladkevich, S.; Gun, J.; Prikhodchenko, P.V.; Lev, O. Green Synthesis of a Nanocrystalline Tin Disulfide-Reduced Graphene Oxide Anode from Ammonium Peroxostannate: A Highly Stable Sodium-Ion Battery Anode. *ACS Sustain. Chem. Eng.* **2020**, *8*, 5485–5494. [[CrossRef](#)]
7. Jeghan, S.M.N.; Lee, G. One-Dimensional Hierarchical Nanostructures of NiCo₂O₄, NiCo₂S₄ and NiCo₂Se₄ with Superior Electrocatalytic Activities toward Efficient Oxygen Evolution Reaction. *Nanotechnology* **2020**, *31*, 295405. [[CrossRef](#)]
8. Iqbal, J.; Jan, T.; Ul-Hassan, S.; Ahmed, I.; Mansoor, Q.; Umair Ali, M.; Abbas, F.; Ismail, M. Facile Synthesis of Zn Doped CuO Hierarchical Nanostructures: Structural, Optical and Antibacterial Properties. *AIP Adv.* **2015**, *5*, 127112. [[CrossRef](#)]
9. Zheng, P.; Dai, Z.; Zhang, Y.; Dinh, K.N.; Zheng, Y.; Fan, H.; Yang, J.; Dangol, R.; Li, B.; Zong, Y.; et al. Scalable Synthesis of SnS₂/S-Doped Graphene Composites for Superior Li/Na-Ion Batteries. *Nanoscale* **2017**, *9*, 14820–14825. [[CrossRef](#)]

10. Wu, L.; Shao, H.; Yang, C.; Feng, X.; Han, L.; Zhou, Y.; Du, W.; Sun, X.; Xu, Z.; Zhang, X.; et al. SnS₂ Nanosheets with rGO Modification as High-Performance Anode Materials for Na-Ion and K-Ion Batteries. *Nanomaterials* **2021**, *11*, 1932. [[CrossRef](#)]
11. Smith, A.T.; LaChance, A.M.; Zeng, S.; Liu, B.; Sun, L. Synthesis, Properties, and Applications of Graphene Oxide/Reduced Graphene Oxide and Their Nanocomposites. *Nano Mater. Sci.* **2019**, *1*, 31–47. [[CrossRef](#)]
12. Tao, H.; Xiong, L.; Zhu, S.; Yang, X.; Zhang, L. Flexible Binder-Free Reduced Graphene Oxide Wrapped Si/Carbon Fibers Paper Anode for High-Performance Lithium Ion Batteries. *Int. J. Hydrogen Energy* **2016**, *41*, 21268–21277. [[CrossRef](#)]
13. Li, H.; He, X.; Kang, Z.; Huang, H.; Liu, Y.; Liu, J.; Lian, S.; Tsang, C.H.A.; Yang, X.; Lee, S.T. Water-Soluble Fluorescent Carbon Quantum Dots and Photocatalyst Design. *Angew. Chem. Int. Ed.* **2010**, *49*, 4430–4434. [[CrossRef](#)]
14. Xiong, Z.; Fuji, M.; Zhou, J. Ultrathin Carbon-Coated Fe₇S₈ Core/Shell Nanosheets towards Superb Na Storage in Both Ether and Ester Electrolyte Systems. *Sustain. Energy Fuels* **2019**, *3*, 2845–2858. [[CrossRef](#)]
15. Mas, N.; Hueso, J.L.; Martinez, G.; Madrid, A.; Mallada, R.; Ortega-Liebana, M.C.; Bueno-Alejo, C.; Santamaria, J. Laser-Driven Direct Synthesis of Carbon Nanodots and Application as Sensitizers for Visible-Light Photocatalysis. *Carbon. N. Y.* **2020**, *156*, 453–462. [[CrossRef](#)]
16. Yan, L.; Li, L.; Ru, X.; Wen, D.; Ding, L.; Zhang, X.; Diao, H.; Qin, Y. Core-Shell, Wire-in-Tube and Nanotube Structures: Carbon-Based Materials by Molecular Layer Deposition for Efficient Microwave Absorption. *Carbon. N. Y.* **2021**, *173*, 145–153. [[CrossRef](#)]
17. Yan, D.; Liu, J.; Zhang, Z.; Wang, Y.; Zhang, M.; Song, D.; Zhang, T.; Liu, J.; He, F.; Wang, J. Dual-Functional Graphene Oxide-Based Nanomaterial for Enhancing the Passive and Active Corrosion Protection of Epoxy Coating. *Compos. B Eng.* **2021**, *222*, 109075. [[CrossRef](#)]
18. Luo, D.; Wang, X.; Zhang, Z.; Gao, D.; Liu, Z.; Chen, J. Enhancement of Photocatalytic Hydrogen Evolution from Dye-Sensitized Amide-Functionalized Carbon Nanospheres by Superior Adsorption Performance. *Int. J. Hydrog. Energy* **2020**, *45*, 30375–30386. [[CrossRef](#)]
19. Kim, Y.; Yang, H.-S.; Yoon, J.; Jun Jo, M.; Ho Youk, J.; Lee, B.-S.; Yu, W.-R. Electrochemical Properties of PVP-Derived Carbon Nanospheres with Various Porosity and Heteroatom Contents in Anode Voltage Range over Full-Cell Operation. *J. Ind. Eng. Chem.* **2022**, *105*, 146–157. [[CrossRef](#)]
20. Liang, L.; Chang, Q.; Cai, T.; Li, N.; Xue, C.; Yang, J.; Hu, S. Combining Carbon Dots with WO_{3-x} Nanodots for Utilizing the Full Spectrum of Solar Radiation in Photocatalysis. *Chem. Eng. J.* **2022**, *428*, 131139. [[CrossRef](#)]
21. Khazaei, Z.; Mahjoub, A.R.; Cheshme Khavar, A.H. One-Pot Synthesis of CuBi Bimetallic Alloy Nanosheets-Supported Functionalized Multiwalled Carbon Nanotubes as Efficient Photocatalyst for Oxidation of Fluoroquinolones. *Appl. Catal. B* **2021**, *297*, 120480. [[CrossRef](#)]
22. Neravathu, D.; Paloly, A.R.; Sajan, P.; Satheesh, M.; Bushiri, M.J. Hybrid Nanomaterial of ZnFe₂O₄/α-Fe₂O₃ Implanted Graphene for Electrochemical Glucose Sensing Application. *Diam. Relat. Mater.* **2020**, *106*, 107852. [[CrossRef](#)]
23. Liu, X.; Zhang, X.; Zheng, J. One-Pot Fabrication of AuNPs-Prussian Blue-Graphene Oxide Hybrid Nanomaterials for Non-Enzymatic Hydrogen Peroxide Electrochemical Detection. *Microchem. J.* **2021**, *160*, 105595. [[CrossRef](#)]
24. Qin, X.; Huang, Y.; Wang, K.; Xu, T.; Li, S.; Zhao, M.; Wang, Y.; Chen, Q. Novel Hexagonal Bi₂O₂CO₃ Porous Nanoplate/Nitrogen-Doped Graphene Nanomaterial Enhanced Electrochemical Properties of Oxygen Reduction Reaction in Acidic Medium for Fuel Cells. *Carbon. N. Y.* **2019**, *152*, 459–473. [[CrossRef](#)]
25. Balakumar, V.; Selvarajan, S.; Baishnisha, A.; Kathiresan, S. In-Situ Growth of TiO₂@B-Doped g-C₃N₄ Core-Shell Nanospheres for Boosts the Photocatalytic Detoxification of Emerging Pollutants with Mechanistic Insight. *Appl. Surf. Sci.* **2022**, *577*, 151924. [[CrossRef](#)]
26. Wu, J.J.; Tao, Y.R.; Wu, Y.; Wu, X.C. Ultrathin SnS₂ Nanosheets of Ultrasonic Synthesis and Their Photoresponses from Ultraviolet to Near-Infrared. *Sens. Actuators B Chem.* **2016**, *231*, 211–217. [[CrossRef](#)]
27. Wei, H.; Hou, C.; Zhang, Y.; Nan, Z. Scalable Low Temperature in Air Solid Phase Synthesis of Porous Flower-like Hierarchical Nanostructure SnS₂ with Superior Performance in the Adsorption and Photocatalytic Reduction of Aqueous Cr(VI). *Sep. Purif. Technol.* **2017**, *189*, 153–161. [[CrossRef](#)]
28. Liu, X.; Sakthivel, R.; Chen, Y.C.; Chang, N.; Dhawan, U.; Li, Y.; Zhao, G.; Lin, C.; Chung, R.J. Tin Disulfide-Graphene Oxide-β-Cyclodextrin Mediated Electro-Oxidation of Melatonin Hormone: An Efficient Platform for Electrochemical Sensing. *J. Mater. Chem. B* **2020**, *8*, 7539–7547. [[CrossRef](#)]
29. Mahmud, S.T.; Mia, R.; Mahmud, S.; Sha, S.; Zhang, R.; Deng, Z.; Yanilmaz, M.; Luo, L.; Zhu, J. Recent Developments of Tin (II) Sulfide/Carbon Composites for Achieving High-Performance Lithium Ion Batteries: A Critical Review. *Nanomaterials* **2022**, *12*, 1246. [[CrossRef](#)]
30. Zhan, S.; Zheng, L.; Xiao, Y.; Zhao, L.D. Phonon and Carrier Transport Properties in Low-Cost and Environmentally Friendly SnS₂: A Promising Thermoelectric Material. *Chem. Mater.* **2020**, *32*, 10348–10356. [[CrossRef](#)]
31. Munn, Z.; Peters, M.D.J.; Stern, C.; Tufanaru, C.; McArthur, A.; Aromataris, E. Systematic Review or Scoping Review? Guidance for Authors When Choosing between a Systematic or Scoping Review Approach. *BMC Med. Res. Methodol.* **2018**, *18*, 1–17. [[CrossRef](#)] [[PubMed](#)]
32. Hayashi, H.; Hakuta, Y. Hydrothermal Synthesis of Metal Oxide Nanoparticles in Supercritical Water. *Materials* **2010**, *3*, 3794–3817. [[CrossRef](#)] [[PubMed](#)]

33. Yahya, R.B.; Hayashi, H.; Nagase, T.; Ebina, T.; Onodera, Y.; Saitoh, N. Hydrothermal Synthesis of Potassium Hexatitanates under Subcritical and Supercritical Water Conditions and Its Application in Photocatalysis. *Chem. Mater.* **2001**, *13*, 842–847. [[CrossRef](#)]
34. Bai, X.; Li, L.; Liu, H.; Tan, L.; Liu, T.; Meng, X. Solvothermal Synthesis of ZnO Nanoparticles and Anti-Infection Application in Vivo. *ACS Appl. Mater. Interfaces* **2015**, *7*, 1308–1317. [[CrossRef](#)]
35. Zhang, Y.C.; Li, J.; Xu, H.Y. One-Step in Situ Solvothermal Synthesis of SnS₂/TiO₂ Nanocomposites with High Performance in Visible Light-Driven Photocatalytic Reduction of Aqueous Cr(VI). *Appl. Catal. B* **2012**, *123–124*, 18–26. [[CrossRef](#)]
36. Vakhrushev, A.Y.; Boitsova, T.B. TiO₂ and TiO₂/Ag Nanofibers: Template Synthesis, Structure, and Photocatalytic Properties. *J. Porous Mater.* **2021**, *28*, 1023–1030. [[CrossRef](#)]
37. Tsukigase, H.; Suzuki, Y.; Berger, M.-H.; Sagawa, T.; Yoshikawa, S. Wet Chemical Synthesis and Self-Assembly of SnS₂ Nanoparticles on TiO₂ for Quantum Dot-Sensitized Solar Cells. *J. Nanosci. Nanotechnol.* **2011**, *11*, 3215–3221. [[CrossRef](#)]
38. Al-Shakban, M.; Al-Dulaimi, N.; Xaba, T.; Raheel, A. Hot Injection Synthesis of Orthorhombic SnS Nanoparticles from Bis(O-n-Propyl)dithiocarbonato)Diphenyltin(IV). *J. Nano Res.* **2021**, *66*, 27–34. [[CrossRef](#)]
39. Liang, Z.; Mu, J.; Mu, Y.; Shi, J.; Hao, W.; Dong, X.; Yu, H. Interface-Mediated Synthesis of Monodisperse ZnS Nanoparticles with Sulfate-Reducing Bacterium Culture. *J. Environ. Sci.* **2013**, *25*, S106–S109. [[CrossRef](#)]
40. Chaki, S.H.; Deshpande, M.P.; Trivedi, D.P.; Tailor, J.P.; Chaudhary, M.D.; Mahato, K. Wet Chemical Synthesis and Characterization of SnS₂ Nanoparticles. *Appl. Nanosci.* **2013**, *3*, 189–195. [[CrossRef](#)]
41. Joseph, A.; Anjitha, C.R.; Aravind, A.; Aneesh, P.M. Structural, Optical and Magnetic Properties of SnS₂ Nanoparticles and Photo Response Characteristics of p-Si/n-SnS₂ Heterojunction Diode. *Appl. Surf. Sci.* **2020**, *528*, 146977. [[CrossRef](#)]
42. Song, H.; Wu, H.; Gao, Y.; Wang, K.; Su, X.; Yan, S.; Shi, Y. Production of SnS₂ Nanostructure as Improved Light-Assisted Electrochemical Water Splitting. *Nanomaterials* **2019**, *9*, 1244. [[CrossRef](#)] [[PubMed](#)]
43. Ullah, S.; Bouich, A.; Ullah, H.; Mari, B.; Mollar, M. Enhanced Optical and Structural Properties of V-Doped Binary SnS₂ Buffer Layer. *Solar. Energy* **2020**, *204*, 654–659. [[CrossRef](#)]
44. Umar, A.; Akhtar, M.S.; Dar, G.N.; Abaker, M.; Al-Hajry, A.; Baskoutas, S. Visible-Light-Driven Photocatalytic and Chemical Sensing Properties of SnS₂ Nanoflakes. *Talanta* **2013**, *114*, 183–190. [[CrossRef](#)] [[PubMed](#)]
45. Yu, J.; Xu, C.Y.; Ma, F.X.; Hu, S.P.; Zhang, Y.W.; Zhen, L. Monodisperse SnS₂ Nanosheets for High-Performance Photocatalytic Hydrogen Generation. *ACS Appl. Mater. Interfaces* **2014**, *6*, 22370–22377. [[CrossRef](#)] [[PubMed](#)]
46. Yang, Z.; Su, C.; Wang, S.; Han, Y.; Chen, X.; Xu, S.; Zhou, Z.; Hu, N.; Su, Y.; Zeng, M. Highly Sensitive NO₂ Gas Sensors Based on Hexagonal SnS₂ Nanoplates Operating at Room Temperature. *Nanotechnology* **2019**, *31*, 075501. [[CrossRef](#)] [[PubMed](#)]
47. Parveen, N.; Ansari, S.A.; Alamri, H.R.; Ansari, M.O.; Khan, Z.; Cho, M.H. Facile Synthesis of SnS₂ Nanostructures with Different Morphologies for High-Performance Supercapacitor Applications. *ACS Omega* **2018**, *3*, 1581–1588. [[CrossRef](#)]
48. Wang, Y.; Zhou, J.; Wu, J.; Chen, F.; Li, P.; Han, N.; Huang, W.; Liu, Y.; Ye, H.; Zhao, F.; et al. Engineering SnS₂ Nanosheet Assemblies for Enhanced Electrochemical Lithium and Sodium Ion Storage. *J. Mater. Chem. A Mater.* **2017**, *5*, 25618–25624. [[CrossRef](#)]
49. Geng, H.; Su, Y.; Wei, H.; Xu, M.; Wei, L.; Yang, Z.; Zhang, Y. Controllable Synthesis and Photoelectric Property of Hexagonal SnS₂ Nanoflakes by Triton X-100 Assisted Hydrothermal Method. *Mater. Lett.* **2013**, *111*, 204–207. [[CrossRef](#)]
50. Liu, G.; Li, Z.; Hasan, T.; Chen, X.; Zheng, W.; Feng, W.; Jia, D.; Zhou, Y.; Hu, P.A. Vertically Aligned Two-Dimensional SnS₂ Nanosheets with a Strong Photon Capturing Capability for Efficient Photoelectrochemical Water Splitting. *J. Mater. Chem. A Mater.* **2017**, *5*, 1989–1995. [[CrossRef](#)]
51. Thangaraju, D.; Marnadu, R.; Santhana, V.; Durairajan, A.; Kathirvel, P.; Chandrasekaran, J.; Jayakumar, S.; Valente, M.A.; Greenidge, D.C. Solvent Influenced Synthesis of Single-Phase SnS₂ Nanosheets for Solution-Processed Photodiode Fabrication. *CrystEngComm* **2020**, *22*, 525–533. [[CrossRef](#)]
52. Du, W.; Deng, D.; Han, Z.; Xiao, W.; Bian, C.; Qian, X. Hexagonal Tin Disulfide Nanoplatelets: A New Photocatalyst Driven by Solar Light. *CrystEngComm* **2011**, *13*, 2071–2076. [[CrossRef](#)]
53. Jana, M.K.; Rajendra, H.B.; Bhattacharyya, A.J.; Biswas, K. Green Ionothermal Synthesis of Hierarchical Nanostructures of SnS₂ and Their Li-Ion Storage Properties. *CrystEngComm* **2014**, *16*, 3994–4000. [[CrossRef](#)]
54. Jiang, X.; Yang, X.; Zhu, Y.; Shen, J.; Fan, K.; Li, C. In Situ Assembly of Graphene Sheets-Supported SnS₂ Nanoplates into 3D Macroporous Aerogels for High-Performance Lithium Ion Batteries. *J Power Sources* **2013**, *237*, 178–186. [[CrossRef](#)]
55. Luo, B.; Hu, Y.; Zhu, X.; Qiu, T.; Zhi, L.; Xiao, M.; Zhang, H.; Zou, M.; Cao, A.; Wang, L. Controllable Growth of SnS₂ Nanostructures on Nanocarbon Surfaces for Lithium-Ion and Sodium-Ion Storage with High Rate Capability. *J. Mater. Chem. A Mater.* **2018**, *6*, 1462–1472. [[CrossRef](#)]
56. Liu, Z.; Xu, J.; Zhao, Y.; An, Y.; Tao, J.; Zhang, F.; Zhang, X. Hexagonal SnS₂ Nanosheets Crosslinked by Bacterial Cellulose Derived Carbon Nanofibers for Fast Sodium Ion Batteries. *J. Alloys Compd.* **2019**, *802*, 269–275. [[CrossRef](#)]
57. Cheng, Y.; Xie, H.; Zhou, L.; Shi, B.; Guo, L.; Huang, J. In-Situ Liquid-Phase Transformation of SnS₂/CNTs Composite from SnO₂/CNTs for High Performance Lithium-Ion Battery Anode. *Appl. Surf. Sci.* **2021**, *566*, 150645. [[CrossRef](#)]
58. Zhai, C.; Du, N.; Zhang, H.; Yu, J.; Yang, D. Multiwalled Carbon Nanotubes Anchored with SnS₂ Nanosheets as High-Performance Anode Materials of Lithium-Ion Batteries. *ACS Appl. Mater. Interfaces* **2011**, *3*, 4067–4074. [[CrossRef](#)]
59. Qu, B.; Ma, C.; Ji, G.; Xu, C.; Xu, J.; Meng, Y.S.; Wang, T.; Lee, J.Y. Layered SnS₂-Reduced Graphene Oxide Composite-A High-Capacity, High-Rate, and Long-Cycle Life Sodium-Ion Battery Anode Material. *Adv. Mater.* **2014**, *26*, 3854–3859. [[CrossRef](#)]

60. Chauhan, H.; Soni, K.; Kumar, M.; Deka, S. Tandem Photocatalysis of Graphene-Stacked SnS₂ Nanodiscs and Nanosheets with Efficient Carrier Separation. *ACS Omega* **2016**, *1*, 127–137. [[CrossRef](#)]
61. Zhang, Z.; Feng, L.; Jing, P.; Hou, X.; Suo, G.; Ye, X.; Zhang, L.; Yang, Y.; Zhai, C. In Situ Construction of Hierarchical Polyaniline/SnS₂@carbon Nanotubes on Carbon Fibers for High-Performance Supercapacitors. *J. Colloid. Interface Sci.* **2021**, *588*, 84–93. [[CrossRef](#)] [[PubMed](#)]
62. Liu, P.; Jin, L.N.; Jin, C.; Zhang, J.N.; Bian, S.W. Synthesis of Hierarchically Porous Silicate-1 and ZSM-5 by Hydrothermal Transformation of SiO₂ Colloid Crystal/Carbon Composites. *Microporous Mesoporous Mater.* **2018**, *262*, 217–226. [[CrossRef](#)]
63. Manikandan, V.S.; Palai, A.K.; Mohanty, S.; Nayak, S.K. Hydrothermally Synthesized Self-Assembled Multi-Dimensional TiO₂/Graphene Oxide Composites with Efficient Charge Transfer Kinetics Fabricated as Novel Photoanode for Dye Sensitized Solar Cell. *J. Alloys Compd.* **2019**, *793*, 400–409. [[CrossRef](#)]
64. Zhang, S.; Zhao, H.; Wu, M.; Yue, L.; Mi, J. One-Pot Solvothermal Synthesis 2D SnS₂/CNTs Hybrid as a Superior Anode Material for Sodium-Ion Batteries. *J. Alloys Compd.* **2018**, *737*, 92–98. [[CrossRef](#)]
65. Shen, C.; Ma, L.; Zheng, M.; Zhao, B.; Qiu, D.; Pan, L.; Cao, J.; Shi, Y. Synthesis and Electrochemical Properties of Graphene-SnS₂ Nanocomposites for Lithium-Ion Batteries. *J. Solid State Electrochem.* **2012**, *16*, 1999–2004. [[CrossRef](#)]
66. Anlin Lazar, K.; Cicily Rigi, V.J.; Divya, D.; Saji, K.J. Effect of Annealing on Structural and Optical Properties of SnS₂ Thin Films Grown by Thermal Evaporation and Post Sulphur Annealing Technique. *IOP Conf. Ser. Mater. Sci. Eng.* **2021**, *1166*, 012004. [[CrossRef](#)]
67. Zhuang, S.; Lee, E.S.; Lei, L.; Nunna, B.B.; Kuang, L.; Zhang, W. Synthesis of Nitrogen-Doped Graphene Catalyst by High-Energy Wet Ball Milling for Electrochemical Systems. *Int. J. Energy Res.* **2016**, *40*, 2136–2149. [[CrossRef](#)]
68. Heidari, M.; Hosseini, S.S.; Omidkhan Nasrin, M.R.; Ghadimi, A. Synthesis and Fabrication of Adsorptive Carbon Nanoparticles (ACNs)/PDMS Mixed Matrix Membranes for Efficient CO₂/CH₄ and C₃H₈/CH₄ Separation. *Sep. Purif. Technol.* **2019**, *209*, 503–515. [[CrossRef](#)]
69. Zhang, Z.; Wen, G. Synthesis and Characterization of Carbon-Encapsulated Magnetite, Martensite and Iron Nanoparticles by High-Energy Ball Milling Method. *Mater. Charact.* **2020**, *167*, 110502. [[CrossRef](#)]
70. Zheng, Y.; Wan, Y.; Chen, J.; Chen, H.; Gao, B. MgO Modified Biochar Produced through Ball Milling: A Dual-Functional Adsorbent for Removal of Different Contaminants. *Chemosphere* **2020**, *243*, 125344. [[CrossRef](#)]
71. Dogrusoz, M.; Demir-Cakan, R. Mechanochemical Synthesis of SnS Anodes for Sodium Ion Batteries. *Int. J. Energy Res.* **2020**, *44*, 10809–10820. [[CrossRef](#)]
72. Lasio, B.; Torre, F.; Orrù, R.; Cao, G.; Cabibbo, M.; Delogu, F. Fabrication of Cu-Graphite Metal Matrix Composites by Ball Milling and Spark Plasma Sintering. *Mater. Lett.* **2018**, *230*, 199–202. [[CrossRef](#)]
73. Li, X.; Yan, S.; Chen, X.; Hong, Q.; Wang, N. Microstructure and Mechanical Properties of Graphene-Reinforced Copper Matrix Composites Prepared by in-Situ CVD, Ball-Milling, and Spark Plasma Sintering. *J. Alloys Compd.* **2020**, *834*, 155182. [[CrossRef](#)]
74. Bai, C.; An, L.; Zhang, J.; Zhang, X.; Zhang, B.; Qiang, L.; Yu, Y.; Zhang, J. Superlow Friction of Amorphous Diamond-like Carbon Films in Humid Ambient Enabled by Hexagonal Boron Nitride Nanosheet Wrapped Carbon Nanoparticles. *Chem. Eng. J.* **2020**, *402*, 126206. [[CrossRef](#)]
75. Kapusta, K.; Drygas, M.; Janik, J.F.; Olejniczak, Z. New Synthesis Route to Kesterite Cu₂ZnSnS₄ Semiconductor Nanocrystalline Powders Utilizing Copper Alloys and a High Energy Ball Milling-Assisted Process. *J. Mater. Res. Technol.* **2020**, *9*, 13320–13331. [[CrossRef](#)]
76. Al-Mamun, M.; Wang, Y.; Liu, P.; Zhong, Y.L.; Yin, H.; Su, X.; Zhang, H.; Yang, H.; Wang, D.; Tang, Z.; et al. One-Step Solid Phase Synthesis of a Highly Efficient and Robust Cobalt Pentlandite Electrocatalyst for the Oxygen Evolution Reaction. *J. Mater. Chem. A Mater.* **2016**, *4*, 18314–18321. [[CrossRef](#)]
77. Zhang, Y.C.; Du, Z.N.; Li, S.Y.; Zhang, M. Novel Synthesis and High Visible Light Photocatalytic Activity of SnS₂ Nanoflakes from SnCl₂·2H₂O and S Powders. *Appl. Catal. B* **2010**, *95*, 153–159. [[CrossRef](#)]
78. Kiruthigaa, G.; Manoharan, C.; Raju, C.; Dhanapandian, S.; Thanikachalam, V. Synthesis and Spectroscopic Analysis of Undoped and Zn Doped SnS₂ Nanostructure by Solid State Reaction Method. *Mater. Sci Semicond. Process.* **2014**, *26*, 533–539. [[CrossRef](#)]
79. Kiruthigaa, G.; Manoharan, C.; Raju, C.; Jayabharathi, J.; Dhanapandian, S. Solid State Synthesis and Spectral Investigations of Nanostructure SnS₂. *Spectrochim. Acta A Mol. Biomol. Spectrosc.* **2014**, *129*, 415–420. [[CrossRef](#)]
80. Xiao, H.; Zhang, Y.C. In Air Synthesis of SnS₂ Nanoplates from Tin, Sulfur and Ammonium Chloride Powders. *Mater. Chem. Phys.* **2008**, *112*, 742–744. [[CrossRef](#)]
81. Wang, S.; Peng, T.; Zhang, Y. NH₄Cl-Assisted in Air, Low Temperature Synthesis of SnS₂ Nanoflakes with High Visible-Light-Activated Photocatalytic Activity. *Mater. Lett.* **2019**, *234*, 361–363. [[CrossRef](#)]
82. Wang, J.; Luo, C.; Mao, J.; Zhu, Y.; Fan, X.; Gao, T.; Mignerey, A.C.; Wang, C. Solid-State Fabrication of SnS₂/C Nanospheres for High-Performance Sodium Ion Battery Anode. *ACS Appl. Mater. Interfaces* **2015**, *7*, 11476–11481. [[CrossRef](#)] [[PubMed](#)]
83. Guan, H.; Zeng, T.; Zhang, C. Improve Electrochemical Performances of SnS₂/C by Destroying the Crystal Structure. *Ionics* **2020**, *26*, 579–588. [[CrossRef](#)]
84. Zhao, H.; Zeng, H.; Wu, Y.; Qi, W.; Zhang, S.; Li, B.; Huang, Y. Facile Ball-Milled Synthesis of SnS₂-Carbon Nanocomposites with Superior Lithium Storage. *Prog. Nat. Sci. Mater. Int.* **2018**, *28*, 676–682. [[CrossRef](#)]

85. Liu, X.J.; Xu, Z.Z.; Xiao, H.; Park, D.K.; Kim, K.W.; Kim, Y.C.; Yeon, S.H.; Ahn, I.S. The Effect of Process Control Agents and Ball to Powder Ratios on the Electrochemical Characteristics of Mechanically Alloyed SnS₂ Anode Materials. *Powder Technol.* **2014**, *259*, 117–124. [[CrossRef](#)]
86. Choi, H.; Lee, S.; Eom, K.S. Facile Phosphorus-Embedding into SnS₂ Using a High-Energy Ball Mill to Improve the Surface Kinetics of P-SnS₂ Anodes for a Li-Ion Battery. *Appl. Surf. Sci.* **2019**, *466*, 578–582. [[CrossRef](#)]
87. Zhu, A.; Qiao, L.; Jia, Z.; Tan, P.; Liu, Y.; Ma, Y.; Pan, J. C-S Bond Induced Ultrafine SnS₂ Dot/Porous g-C₃N₄ Sheet 0D/2D Heterojunction: Synthesis and Photocatalytic Mechanism Investigation. *Dalton Trans.* **2017**, *46*, 17032–17040. [[CrossRef](#)]
88. Fan, Z.; Luan, J.; Zhu, C.; Liu, F. Depositing Ag₂S Quantum Dots as Electron Mediators in SnS₂/g-C₃N₄ Nanosheet Composites for Constructing Z-Scheme Heterojunction with Enhanced Photocatalytic Performance. *Mater. Res. Bull.* **2021**, *133*, 111045. [[CrossRef](#)]
89. Wei, W.; Jia, F.F.; Wang, K.F.; Qu, P. SnS₂/Graphene Nanocomposite: A High Rate Anode Material for Lithium Ion Battery. *Chin. Chem. Lett.* **2017**, *28*, 324–328. [[CrossRef](#)]
90. Chen, H.; Zhang, B.; Zhang, J.; Yu, W.; Zheng, J.; Ding, Z.; Li, H.; Ming, L.; Bengono, D.A.M.; Chen, S.; et al. In-Situ Grown SnS₂ Nanosheets on RGO as an Advanced Anode Material for Lithium and Sodium Ion Batteries. *Front. Chem.* **2018**, *6*, 629. [[CrossRef](#)]
91. Yella, A.; Mugnaioli, E.; Therese, H.A.; Panthöfer, M.; Kolb, U.; Tremel, W. Synthesis of Fullerene- and Nanotube-Like SnS₂ Nanoparticles and Sn/S/Carbon Nanocomposites. *Chem. Mater.* **2009**, *21*, 2474–2481. [[CrossRef](#)]
92. Xia, J.; Jiang, K.; Xie, J.; Guo, S.; Liu, L.; Zhang, Y.; Nie, S.; Yuan, Y.; Yan, H.; Wang, X. Tin Disulfide Embedded in N-, S-Doped Carbon Nanofibers as Anode Material for Sodium-Ion Batteries. *Chem. Eng. J.* **2019**, *359*, 1244–1251. [[CrossRef](#)]
93. Wang, J.G.; Sun, H.; Liu, H.; Jin, D.; Liu, X.; Li, X.; Kang, F. Triaxial Nanocables of Conducting Polypyrrole@SnS₂@Carbon Nanofiber Enabling Significantly Enhanced Li-Ion Storage. *ACS Appl. Mater. Interfaces* **2018**, *10*, 13581–13587. [[CrossRef](#)] [[PubMed](#)]
94. Li, H.; Zhou, M.; Li, W.; Wang, K.; Cheng, S.; Jiang, K. Layered SnS₂ Cross-Linked by Carbon Nanotubes as a High Performance Anode for Sodium Ion Batteries. *RSC Adv.* **2016**, *6*, 35197–35202. [[CrossRef](#)]
95. Sun, H.; Ahmad, M.; Luo, J.; Shi, Y.; Shen, W.; Zhu, J. SnS₂ Nanoflakes Decorated Multiwalled Carbon Nanotubes as High Performance Anode Materials for Lithium-Ion Batteries. *Mater. Res. Bull.* **2014**, *49*, 319–324. [[CrossRef](#)]
96. Ren, Z.; Wen, J.; Liu, W.; Jiang, X.; Dong, Y.; Guo, X.; Zhao, Q.; Ji, G.; Wang, R.; Hu, N.; et al. Rational Design of Layered SnS₂ on Ultralight Graphene Fiber Fabrics as Binder-Free Anodes for Enhanced Practical Capacity of Sodium-Ion Batteries. *Nanomicro. Lett.* **2019**, *11*, 66. [[CrossRef](#)]
97. Jin, X.; Huang, H.; Wu, A.; Gao, S.; Lei, M.; Zhao, J.; Gao, X.; Cao, G. Inverse Capacity Growth and Pocket Effect in SnS₂ Semifilled Carbon Nanotube Anode. *ACS Nano* **2018**, *12*, 8037–8047. [[CrossRef](#)]
98. Lu, X.; Liu, D.; Han, T.; Zhu, M.; Ryu, S.O.; Huang, J. A Facile Synthesis of Sandwich-Structured SnS₂@reduced Graphene Oxide with High Performance for Lithium-Ion Battery Anode. *J. Alloys Compd.* **2018**, *765*, 1061–1071. [[CrossRef](#)]
99. Fan, L.; Li, X.; Song, X.; Hu, N.; Xiong, D.; Koo, A.; Sun, X. Promising Dual-Doped Graphene Aerogel/SnS₂ Nanocrystal Building High Performance Sodium Ion Batteries. *ACS Appl. Mater. Interfaces* **2018**, *10*, 2637–2648. [[CrossRef](#)]
100. Jiang, Y.; Wei, M.; Feng, J.; Ma, Y.; Xiong, S. Enhancing the Cycling Stability of Na-Ion Batteries by Bonding SnS₂ Ultrafine Nanocrystals on Amino-Functionalized Graphene Hybrid Nanosheets. *Energy Environ. Sci.* **2016**, *9*, 1430–1438. [[CrossRef](#)]
101. Prikhodchenko, P.V.; Yu, D.Y.W.; Batabyal, S.K.; Uvarov, V.; Gun, J.; Sladkevich, S.; Mikhaylov, A.A.; Medvedev, A.G.; Lev, O. Nanocrystalline Tin Disulfide Coating of Reduced Graphene Oxide Produced by the Peroxostannate Deposition Route for Sodium Ion Battery Anodes. *J. Mater. Chem. A Mater.* **2014**, *2*, 8431–8437. [[CrossRef](#)]
102. Li, X.; Sun, X.; Gao, Z.; Hu, X.; Ling, R.; Cai, S.; Zheng, C.; Hu, W. A Simple One-Pot Strategy for Synthesizing Ultrafine SnS₂ Nanoparticle/Graphene Composites as Anodes for Lithium/Sodium-Ion Batteries. *ChemSusChem* **2018**, *11*, 1549–1557. [[CrossRef](#)] [[PubMed](#)]
103. Shown, I.; Samireddi, S.; Chang, Y.C.; Putikam, R.; Chang, P.H.; Sabbah, A.; Fu, F.Y.; Chen, W.F.; Wu, C.I.; Yu, T.Y.; et al. Carbon-Doped SnS₂ Nanostructure as a High-Efficiency Solar Fuel Catalyst under Visible Light. *Nat. Commun.* **2018**, *9*, 169. [[CrossRef](#)] [[PubMed](#)]
104. Zheng, S.; Li, Y.; Hao, J.; Fang, H.; Yuan, Y.; Tsai, H.S.; Sun, Q.; Wan, P.; Zhang, X.; Wang, Y. Hierarchical Assembly of Graphene-Bridged SnO₂-RGO/SnS₂ Heterostructure with Interfacial Charge Transfer Highway for High-Performance NO₂ Detection. *Appl. Surf. Sci.* **2021**, *568*, 150926. [[CrossRef](#)]
105. Youn, D.H.; Stauffer, S.K.; Xiao, P.; Park, H.; Nam, Y.; Dolocan, A.; Henkelman, G.; Heller, A.; Mullins, C.B. Simple Synthesis of Nanocrystalline Tin Sulfide/N-Doped Reduced Graphene Oxide Composites as Lithium Ion Battery Anodes. *ACS Nano* **2016**, *10*, 10778–10788. [[CrossRef](#)]
106. Fang, F.; Li, H.; Yao, H.; Jiang, K.; Liu, Z.; Lin, C.; Chen, F.; Wang, Y.; Liu, L. Two-Dimensional Hybrid Composites of SnS₂ Nanosheets Array Film with Graphene for Enhanced Photoelectric Performance. *Nanomaterials* **2019**, *9*, 1122. [[CrossRef](#)]
107. Zhang, D.; Zong, X.; Wu, Z. Fabrication of Tin Disulfide/Graphene Oxide Nanoflower on Flexible Substrate for Ultrasensitive Humidity Sensing with Ultralow Hysteresis and Good Reversibility. *Sens. Actuators B Chem.* **2019**, *287*, 398–407. [[CrossRef](#)]
108. Zeng, L.; Zhang, L.; Liu, X.; Zhang, C. SnS₂ Nanocrystalline-Anchored Three-Dimensional Graphene for Sodium Batteries with Improved Rate Performance. *Nanomaterials* **2020**, *10*, 2336. [[CrossRef](#)]
109. Zhang, Z.; Jiang, L.; Wu, D.; Liang, F.; Li, X.; Rui, Y.; Tang, B. A Novel SnS₂ Nanomaterial Based on Nitrogen-Doped Cubic-like Carbon Skeleton with Excellent Lithium Storage. *J. Alloys Compd.* **2021**, *883*, 160834. [[CrossRef](#)]

110. Li, X.; Zhao, Y.; Yao, Q.; Guan, L. Encapsulating SnS₂ Nanosheets into Hollow Carbon Sphere: A Yolk-Shell SnS₂@C Composite with Enhanced Sodium Storage Performance. *Electrochim. Acta* **2018**, *270*, 8. [[CrossRef](#)]
111. Ren, Y.; Wang, J.; Huang, X.; Ding, J. Three-Dimensional SnS₂ Flowers/Carbon Nanotubes Network: Extraordinary Rate Capacity for Sodium-Ion Battery. *Mater. Lett.* **2017**, *186*, 57–61. [[CrossRef](#)]
112. Li, S.; Zhao, Z.; Li, C.; Liu, Z.; Li, D. SnS₂@C Hollow Nanospheres with Robust Structural Stability as High-Performance Anodes for Sodium Ion Batteries. *Nanomicro. Lett.* **2019**, *11*, 14. [[CrossRef](#)] [[PubMed](#)]
113. Shi, Y.; Sun, L.; Zhang, Y.; Si, H.; Sun, C.; Gu, J.; Gong, Y.; Li, X.; Zhang, Y. SnS₂ Nanodots Decorated on RGO Sheets with Enhanced Pseudocapacitive Performance for Asymmetric Supercapacitors. *J. Alloys. Compd.* **2021**, *853*, 156903. [[CrossRef](#)]
114. Xu, Y.; Zhou, Y.; Guo, J.; Zhang, S.; Lu, Y. Preparation of SnS₂/g-C₃N₄ Composite as the Electrode Material for Supercapacitor. *J. Alloys Compd.* **2019**, *806*, 343–349. [[CrossRef](#)]
115. Srivastava, R.R.; Singh, V.K.; Srivastava, A. Facile Synthesis of Highly Fluorescent Water-Soluble SnS₂ QDs for Effective Detection of Fe³⁺ and Unveiling Its Fluorescence Quenching Mechanism. *Opt. Mater.* **2020**, *109*, 110337. [[CrossRef](#)]
116. Fu, X.; Ilanchezhian, P.; Mohan Kumar, G.; Cho, H.D.; Zhang, L.; Chan, A.S.; Lee, D.J.; Panin, G.N.; Kang, T.W. Tunable UV-Visible Absorption of SnS₂ Layered Quantum Dots Produced by Liquid Phase Exfoliation. *Nanoscale* **2017**, *9*, 1820–1826. [[CrossRef](#)]
117. Lei, Y.M.; Zhou, J.; Chai, Y.Q.; Zhuo, Y.; Yuan, R. SnS₂ Quantum Dots as New Emitters with Strong Electrochemiluminescence for Ultrasensitive Antibody Detection. *Anal. Chem.* **2018**, *90*, 12270–12277. [[CrossRef](#)]
118. Tu, J.R.; Shi, X.F.; Lu, H.W.; Yang, N.X.; Yuan, Y.J. Facile Fabrication of SnS₂ Quantum Dots for Photoreduction of Aqueous Cr(VI). *Mater. Lett.* **2016**, *185*, 303–306. [[CrossRef](#)]
119. Srivastava, R.R.; Mishra, H.; Singh, V.K.; Vikram, K.; Srivastava, R.K.; Srivastava, S.K.; Srivastava, A. PH Dependent Luminescence Switching of Tin Disulfide Quantum Dots. *J. Lumin.* **2019**, *213*, 401–408. [[CrossRef](#)]
120. Tan, F.; Qu, S.; Wu, J.; Liu, K.; Zhou, S.; Wang, Z. Preparation of SnS₂ Colloidal Quantum Dots and Their Application in Organic/Inorganic Hybrid Solar Cells. *Nanoscale Res. Lett.* **2011**, *6*, 298. [[CrossRef](#)]
121. Lin, Y.T.; Shi, J.B.; Chen, Y.C.; Chen, C.J.; Wu, P.F. Synthesis and Characterization of Tin Disulfide (SnS₂) Nanowires. *Nanoscale Res. Lett.* **2009**, *4*, 694–698. [[CrossRef](#)] [[PubMed](#)]
122. Zhao, E.; Gao, L.; Yang, S.; Wang, L.; Cao, J.; Ma, T. In Situ Fabrication of 2D SnS₂ Nanosheets as a New Electron Transport Layer for Perovskite Solar Cells. *Nano. Res.* **2018**, *11*, 5913–5923. [[CrossRef](#)]
123. Li, Q.; Wei, A.; Guo, Z.; Liu, J.; Zhao, Y.; Xiao, Z. Chemical Vapor Deposition of Two-Dimensional SnS₂ Nanoflakes and Flower-Shaped SnS₂. *J. Mater. Sci. Mater. Electron.* **2018**, *29*, 16057–16063. [[CrossRef](#)]
124. Qin, Z.; Xu, K.; Yue, H.; Wang, H.; Zhang, J.; Ouyang, C.; Xie, C.; Zeng, D. Enhanced Room-Temperature NH₃ Gas Sensing by 2D SnS₂ with Sulfur Vacancies Synthesized by Chemical Exfoliation. *Sens. Actuators B Chem.* **2018**, *262*, 771–779. [[CrossRef](#)]
125. Sun, W.; Rui, X.; Yang, D.; Sun, Z.; Li, B.; Zhang, W.; Zong, Y.; Madhavi, S.; Dou, S.; Yan, Q. Two-Dimensional Tin Disulfide Nanosheets for Enhanced Sodium Storage. *ACS Nano*. **2015**, *9*, 11371–11381. [[CrossRef](#)]
126. Liu, G.; Li, Z.; Chen, X.; Zheng, W.; Feng, W.; Dai, M.; Jia, D.; Zhou, Y.; Hu, P. Non-Planar Vertical Photodetectors Based on Free Standing Two-Dimensional SnS₂ Nanosheets. *Nanoscale* **2017**, *9*, 9167–9174. [[CrossRef](#)]
127. Guan, D.; Li, J.; Gao, X.; Xie, Y.; Yuan, C. Growth Characteristics and Influencing Factors of 3D Hierarchical Flower-like SnS₂ Nanostructures and Their Superior Lithium-Ion Intercalation Performance. *J. Alloys Compd.* **2016**, *658*, 190–197. [[CrossRef](#)]
128. Liu, D.; Tang, Z.; Zhang, Z. Nanoplates-Assembled SnS₂ Nanoflowers for Ultrasensitive Ppb-Level NO₂ Detection. *Sens. Actuators B Chem.* **2018**, *273*, 473–479. [[CrossRef](#)]
129. Wu, Q.; Jiao, L.; Du, J.; Yang, J.; Guo, L.; Liu, Y.; Wang, Y.; Yuan, H. One-Pot Synthesis of Three-Dimensional SnS₂ Hierarchitectures as Anode Material for Lithium-Ion Batteries. *J. Power Sources* **2013**, *239*, 89–93. [[CrossRef](#)]
130. Xiong, Y.; Xu, W.; Ding, D.; Lu, W.; Zhu, L.; Zhu, Z.; Wang, Y.; Xue, Q. Ultra-Sensitive NH₃ Sensor Based on Flower-Shaped SnS₂ Nanostructures with Sub-Ppm Detection Ability. *J. Hazard Mater.* **2018**, *341*, 159–167. [[CrossRef](#)]
131. Zai, J.; Wang, K.; Su, Y.; Qian, X.; Chen, J. High Stability and Superior Rate Capability of Three-Dimensional Hierarchical SnS₂ Microspheres as Anode Material in Lithium Ion Batteries. *J. Power Sources* **2011**, *196*, 3650–3654. [[CrossRef](#)]
132. Shi, W.; Huo, L.; Wang, H.; Zhang, H.; Yang, J.; Wei, P. Hydrothermal Growth and Gas Sensing Property of Flower-Shaped SnS₂ Nanostructures. *Nanotechnology* **2006**, *17*, 2918–2924. [[CrossRef](#)]
133. Ahsan, M.A.; He, T.; Eid, K.; Abdullah, A.M.; Curry, M.L.; Du, A.; Puente Santiago, A.R.; Echegoyen, L.; Noveron, J.C. Tuning the Intermolecular Electron Transfer of Low-Dimensional and Metal-Free BCN/C60 Electrocatlysts via Interfacial Defects for Efficient Hydrogen and Oxygen Electrochemistry. *J. Am. Chem. Soc.* **2021**, *143*, 1203–1215. [[CrossRef](#)]
134. Chen, D.; Huang, S.; Huang, R.; Zhang, Q.; Le, T.T.; Cheng, E.; Yue, R.; Hu, Z.; Chen, Z. Electron Beam-Induced Microstructural Evolution of SnS₂ Quantum Dots Assembled on N-Doped Graphene Nanosheets with Enhanced Photocatalytic Activity. *Adv. Mater. Interfaces* **2019**, *6*, 1801759. [[CrossRef](#)]
135. Kong, D.; He, H.; Song, Q.; Wang, B.; Yang, Q.H.; Zhi, L. A Novel SnS₂@graphene Nanocable Network for High-Performance Lithium Storage. *RSC Adv.* **2014**, *4*, 23372–23376. [[CrossRef](#)]
136. Liu, Y.; Yu, X.Y.; Fang, Y.; Zhu, X.; Bao, J.; Zhou, X.; Lou, X.W. (David) Confining SnS₂ Ultrathin Nanosheets in Hollow Carbon Nanostructures for Efficient Capacitive Sodium Storage. *Joule* **2018**, *2*, 725–735. [[CrossRef](#)]
137. Moradian, R.; Astinchap, B. Synthesis and Control Size of SnS₂ Nanoparticles on the Surface Multi-Walled Carbon Nanotubes. *Nano* **2010**, *5*, 139–142. [[CrossRef](#)]

138. Ma, Z.; Wang, Y.; Yang, Y.; Yousaf, M.; Zou, M.; Cao, A.; Han, R.P.S. Flexible Hybrid Carbon Nanotube Sponges Embedded with SnS₂ from Tubular Nanosheaths to Nanosheets as Free-Standing Anodes for Lithium-Ion Batteries. *RSC Adv.* **2016**, *6*, 30098–30105. [[CrossRef](#)]
139. Li, H.; Zhang, B.; Wang, X.; Zhang, J.; An, T.; Ding, Z.; Yu, W.; Tong, H. Heterostructured SnO₂-SnS₂@C Embedded in Nitrogen-Doped Graphene as a Robust Anode Material for Lithium-Ion Batteries. *Front. Chem.* **2019**, *7*, 339. [[CrossRef](#)]
140. Jiang, Y.; Song, D.; Wu, J.; Wang, Z.; Huang, S.; Xu, Y.; Chen, Z.; Zhao, B.; Zhang, J. Sandwich-like SnS₂/Graphene/SnS₂ with Expanded Interlayer Distance as High-Rate Lithium/Sodium-Ion Battery Anode Materials. *ACS Nano* **2019**, *13*, 9100–9111. [[CrossRef](#)]
141. Lonkar, S.P.; Pillai, V.V.; Patole, S.P.; Alhassan, S.M. Scalable in Situ Synthesis of 2D-2D-Type Graphene-Wrapped SnS₂ Nanohybrids for Enhanced Supercapacitor and Electrocatalytic Applications. *ACS Appl. Energy Mater.* **2020**, *3*, 4995–5005. [[CrossRef](#)]
142. Modarres, M.H.; Lim, J.H.-W.; George, C.; Volder, M. De Evolution of RGO-SnS₂ Hybrid Nanoparticle Electrodes in Li-Ion Batteries. *J. Phys. Chem. C* **2017**, *121*, 13018–13024. [[CrossRef](#)]
143. Luo, B.; Fang, Y.; Wang, B.; Zhou, J.; Song, H.; Zhi, L. Two Dimensional Graphene-SnS₂ Hybrids with Superior Rate Capability for Lithium Ion Storage. *Energy Environ. Sci.* **2012**, *5*, 5226–5230. [[CrossRef](#)]
144. Shi, X.; Yang, Z.; Liu, Y.; Tang, Y.; Liu, Y.; Gao, S.; Yang, Y.; Chen, X.; Zhong, Y.; Wu, Z.; et al. Three-Dimensional SnS₂ Nanoarrays with Enhanced Lithium-Ion Storage Properties. *ChemElectroChem* **2020**, *7*, 4484–4491. [[CrossRef](#)]
145. Jiang, M.; Han, T.; Zhang, X. Hollow C@SnS₂/SnS Nanocomposites: High Efficient Oxygen Evolution Reaction Catalysts. *J. Colloid Interface Sci* **2021**, *583*, 149–156. [[CrossRef](#)]
146. FENG, Q.M.; QIN, L.; ZHANG, P.; LI, D.; LIU, M.K.; WANG, P. Ratiometric Electrochemical Detection of MicroRNA Based on Construction of A Hierarchical C@SnS₂ Nanoflower Sensing Interface. *Chin. J. Anal. Chem.* **2021**, *49*, 21020–21028. [[CrossRef](#)]
147. Kamali, K. UV Excited Enhanced Raman Scattering on Carbon-Doped SnS₂ Nanoflowers. *Mater. Res. Bull.* **2022**, *150*, 111757. [[CrossRef](#)]
148. Deng, W.; Chen, X.; Liu, Z.; Hu, A.; Tang, Q.; Li, Z.; Xiong, Y. Three-Dimensional Structure-Based Tin Disulfide/Vertically Aligned Carbon Nanotube Arrays Composites as High-Performance Anode Materials for Lithium Ion Batteries. *J. Power Sources* **2015**, *277*, 131–138. [[CrossRef](#)]
149. Xu, H.; Peng, C.; Yan, Y.; Dong, F.; Sun, H.; Yang, J.; Zheng, S. “All-In-One” Integrated Ultrathin SnS₂@3D Multichannel Carbon Matrix Power High-Areal-Capacity Lithium Battery Anode. *Carbon. Energy* **2019**, *1*, 276–288. [[CrossRef](#)]
150. Gao, S.; Liu, Z.; Yang, L.; Shao, J.; Qu, Q.; Wu, Y.; Adelhelm, P.; Holze, R. Fabrication of S,N-Doped Carbon-Coated SnS₂/SnS Heterostructures Supported by Hollow Carbon Microspheres for Sodium-Ion Storage. *J. Electrochem. Soc.* **2021**, *168*, 050527. [[CrossRef](#)]
151. Muanchan, P.; Kurose, T.; Ito, H. Replication and Thermal Properties of One-Dimensional Composite Nanostructures with Enhanced Mechanical Robustness. *J. Electrochem. Soc.* **2019**, *166*, 3282–3289. [[CrossRef](#)]
152. Wang, X.; Liu, X.; Wang, G.; Xia, Y.; Wang, H. One-Dimensional Hybrid Nanocomposite of High-Density Monodispersed Fe₃O₄ Nanoparticles and Carbon Nanotubes for High-Capacity Storage of Lithium and Sodium. *J. Mater. Chem. A Mater.* **2016**, *4*, 18532–18542. [[CrossRef](#)]
153. Mai, L.; Sheng, J.; Xu, L.; Tan, S.; Meng, J. One-Dimensional Hetero-Nanostructures for Rechargeable Batteries. *Acc. Chem. Res.* **2018**, *51*, 950–959. [[CrossRef](#)]
154. Du, N.; Zhang, H.; Yang, D. One-Dimensional Hybrid Nanostructures: Synthesis via Layer-by-Layer Assembly and Applications. *Nanoscale* **2012**, *4*, 5517–5526. [[CrossRef](#)]
155. Wei, Q.; Xiong, F.; Tan, S.; Huang, L.; Lan, E.H.; Dunn, B.; Mai, L. Porous One-Dimensional Nanomaterials: Design, Fabrication and Applications in Electrochemical Energy Storage. *Adv. Mater.* **2017**, *29*, 1602300. [[CrossRef](#)]
156. Jun, W.; Bing, C.; Qingqing, L.; Ailin, H.; Xiaoying, L.; Qi, J. Preparing a Composite Including SnS₂, Carbon Nanotubes and S and Using as Cathode Material of Lithium-Sulfur Battery. *Scr. Mater.* **2020**, *177*, 208–213. [[CrossRef](#)]
157. Jiang, S.; Chen, M.; Wang, X.; Zeng, P.; Li, Y.; Liu, H.; Li, X.; Huang, C.; Shu, H.; Luo, Z.; et al. A Tin Disulfide Nanosheet Wrapped with Interconnected Carbon Nanotube Networks for Application of Lithium Sulfur Batteries. *Electrochim. Acta* **2019**, *313*, 151–160. [[CrossRef](#)]
158. Chen, G.; Yao, X.; Cao, Q.; Ding, S.; He, J.; Wang, S. Flexible Free-Standing SnS₂/Carbon Nanofibers Anode for High Performance Sodium-Ion Batteries. *Mater. Lett.* **2019**, *234*, 121–124. [[CrossRef](#)]
159. Liu, J.; Chen, X.; Zeng, L.; He, X.; Liu, J.; Huang, B.; Xiao, L.; Qian, Q.; Wei, M.; Chen, Q. SnS₂ Nanosheets Anchored on Porous Carbon Fibers for High Performance of Sodium-Ion Batteries. *J. Electroanal. Chem.* **2020**, *862*, 114021. [[CrossRef](#)]
160. Zhang, G.; Chen, D.; Li, N.; Xu, Q.; Li, H.; He, J.; Lu, J. SnS₂/SnO₂ Heterostructured Nanosheet Arrays Grown on Carbon Cloth for Efficient Photocatalytic Reduction of Cr(VI). *J. Colloid. Interface Sci.* **2018**, *514*, 306–315. [[CrossRef](#)]
161. Xu, W.; Zhao, K.; Zhang, L.; Xie, Z.; Cai, Z.; Wang, Y. SnS₂@Graphene Nanosheet Arrays Grown on Carbon Cloth as Freestanding Binder-Free Flexible Anodes for Advanced Sodium Batteries. *J Alloys. Compd.* **2016**, *654*, 357–362. [[CrossRef](#)]
162. Wang, D.; Yan, X.; Zhou, C.; Wang, J.; Yuan, X.; Jiang, H.; Zhu, Y.; Cheng, X.; Li, R. A Free-Standing Electrode Based on 2D SnS₂ Nanoplates@3D Carbon Foam for High Performance Supercapacitors. *Int. J. Energy Res.* **2020**, *44*, 8542–8554. [[CrossRef](#)]
163. Wu, Y.Q.; Yang, Y.; Pu, H.; Gao, R.Z.; Meng, W.J.; Yang, H.X.; Zhao, D.L. SnS₂ Nanoparticle-Integrated Graphene Nanosheets as High-Performance and Cycle-Stable Anodes for Lithium and Sodium Storage. *J. Alloys Compd.* **2020**, *822*, 153686. [[CrossRef](#)]

164. Sathish, M.; Mitani, S.; Tomai, T.; Honma, I. Ultrathin SnS₂ Nanoparticles on Graphene Nanosheets: Synthesis, Characterization, and Li-Ion Storage Applications. *J. Phys. Chem. C* **2012**, *116*, 12475–12481. [[CrossRef](#)]
165. Ye, J.; Qi, L.; Liu, B.; Xu, C. Facile Preparation of Hexagonal Tin Sulfide Nanoplates Anchored on Graphene Nanosheets for Highly Efficient Sodium Storage. *J. Colloid. Interface Sci.* **2018**, *513*, 188–197. [[CrossRef](#)]
166. Hu, Y.; Ren, X.; Qiao, H.; Huang, Z.; Qi, X.; Zhong, J. Exploring Co-Catalytic Graphene Frameworks for Improving Photocatalytic Activity of Tin Disulfide Nanoplates. *Solar Energy* **2017**, *157*, 905–910. [[CrossRef](#)]
167. Lee, W.; Liu, Y.; Lee, Y.; Sharma, B.K.; Shinde, S.M.; Kim, S.D.; Nan, K.; Yan, Z.; Han, M.; Huang, Y.; et al. Two-Dimensional Materials in Functional Three-Dimensional Architectures with Applications in Photodetection and Imaging. *Nat. Commun.* **2018**, *9*, 1417. [[CrossRef](#)]
168. Guan, D.; Li, J.; Gao, X.; Yuan, C. Carbon Nanotube-Assisted Growth of Single-/Multi-Layer SnS₂ and SnO₂ Nanoflakes for High-Performance Lithium Storage. *RSC Adv.* **2015**, *5*, 58514–58521. [[CrossRef](#)]
169. Tang, H.; Qi, X.; Han, W.; Ren, L.; Liu, Y.; Wang, X.; Zhong, J. SnS₂ Nanoplates Embedded in 3D Interconnected Graphene Network as Anode Material with Superior Lithium Storage Performance. *Appl. Surf. Sci.* **2015**, *355*, 7–13. [[CrossRef](#)]
170. Zhang, Q.; Sun, Y.; Zhang, X.; Guo, J. 3D Architecture Constructed by 2D SnS₂-Graphene Hybrids towards Large and Fast Lithium Storage. *Mater. Lett.* **2016**, *185*, 311–314. [[CrossRef](#)]
171. Liu, H.; Wei, C.; Ai, Z.; Li, M.; Xu, M.; Ma, C.; Shi, J. The Positive Effect of 3D Interpenetrating Network Porous Structure by Carbon Membranes on Alleviating the Volume Expansion of SnS₂ Nanosheets for Enhancing Lithium and Sodium Storage. *Colloids Surf. A Physicochem. Eng. Asp.* **2021**, *610*, 125937. [[CrossRef](#)]
172. Ren, Y.; Lv, W.; Wen, F.; Xiang, J.; Liu, Z. Microwave Synthesis of SnS₂ Nanoflakes Anchored Graphene Foam for Flexible Lithium-Ion Battery Anodes with Long Cycling Life. *Mater. Lett.* **2016**, *174*, 24–27. [[CrossRef](#)]
173. Zheng, J.; Xiong, X.; Wang, G.; Lin, Z.; Ou, X.; Yang, C.; Liu, M. SnS₂ Nanoparticles Anchored on Three-Dimensional Reduced Graphene Oxide as a Durable Anode for Sodium Ion Batteries. *Chem. Eng. J.* **2018**, *339*, 78–84. [[CrossRef](#)]
174. Tang, H.; Qi, X.; Zhang, Z.; Ai, G.; Liu, Y.; Huang, Z.; Zhong, J. Simple Self-Assembly of SnS₂ Entrapped Graphene Aerogel and Its Enhanced Lithium Storage Performance. *Ceram. Int.* **2016**, *42*, 6572–6580. [[CrossRef](#)]
175. Nishiyama, H.; Yamada, T.; Nakabayashi, M.; Maehara, Y.; Yamaguchi, M.; Kuromiya, Y.; Nagatsuma, Y.; Tokudome, H.; Akiyama, S.; Watanabe, T.; et al. Photocatalytic Solar Hydrogen Production from Water on a 100-M² Scale. *Nature* **2021**, *598*, 304–307. [[CrossRef](#)]
176. Jin, S.-E.; Jin, J.E.; Hwang, W.; Hong, S.W. Photocatalytic Antibacterial Application of Zinc Oxide Nanoparticles and Self-Assembled Networks under Dual UV Irradiation for Enhanced Disinfection. *Int. J. Nanomed.* **2019**, *14*, 1737. [[CrossRef](#)]
177. Kong, H.; Song, J.; Jang, J. Photocatalytic Antibacterial Capabilities of TiO₂–Biocidal Polymer Nanocomposites Synthesized by a Surface-Initiated Photopolymerization. *Environ. Sci. Technol.* **2010**, *44*, 5672–5676. [[CrossRef](#)]
178. Zare, M.; Namratha, K.; Alghamdi, S.; Mohammad, Y.H.E.; Hezam, A.; Zare, M.; Drmosh, Q.A.; Byrappa, K.; Chandrashekar, B.N.; Ramakrishna, S.; et al. Novel Green Biomimetic Approach for Synthesis of ZnO-Ag Nanocomposite; Antimicrobial Activity against Food-Borne Pathogen, Biocompatibility and Solar Photocatalysis. *Sci. Rep.* **2019**, *9*, 8303. [[CrossRef](#)]
179. Šuligoj, A.; Štangar, U.; Tušar, N. Photocatalytic Air-Cleaning Using TiO₂ Nanoparticles in Porous Silica Substrate. *Chem. Pap.* **2014**, *68*, 1265–1272. [[CrossRef](#)]
180. Fónagy, O.; Szabó-Bárdos, E.; Horváth, O. 1,4-Benzoquinone and 1,4-Hydroquinone Based Determination of Electron and Superoxide Radical Formed in Heterogeneous Photocatalytic Systems. *J. Photochem. Photobiol. A Chem.* **2021**, *407*, 113057. [[CrossRef](#)]
181. Wang, J.; Wang, C.; Guo, H.; Ye, T.; Liu, Y.; Cheng, X.; Li, W.; Yang, B.; Du, E. Crucial Roles of Oxygen and Superoxide Radical in Bisulfite-Activated Persulfate Oxidation of Bisphenol AF: Mechanisms, Kinetics and DFT Studies. *J. Hazard. Mater.* **2020**, *391*, 122228. [[CrossRef](#)] [[PubMed](#)]
182. Tahir, M.B.; Rafique, M.; Rafique, M.S.; Nawaz, T.; Rizwan, M.; Tanveer, M. Photocatalytic Nanomaterials for Degradation of Organic Pollutants and Heavy Metals. In *Nanotechnology and Photocatalysis for Environmental Applications*; Elsevier Inc.: Amsterdam, The Netherlands, 2020; pp. 119–138.
183. Yasin, S.A.; Abbas, J.A.; Ali, M.M.; Saeed, I.A.; Ahmed, I.H. Methylene Blue Photocatalytic Degradation by TiO₂ Nanoparticles Supported on PET Nanofibres. *Mater. Today Proc.* **2020**, *20*, 482–487. [[CrossRef](#)]
184. Shanmugaratnam, S.; Selvaratnam, B.; Baride, A.; Koodali, R.; Ravirajan, P.; Velauthapillai, D.; Shivatharsiny, Y. SnS₂/TiO₂ Nanocomposites for Hydrogen Production and Photodegradation under Extended Solar Irradiation. *Catalysts* **2021**, *11*, 589. [[CrossRef](#)]
185. Fakhri, A.; Behrouz, S. Assessment of SnS₂ Nanoparticles Properties for Photocatalytic and Antibacterial Applications. *Solar Energy* **2015**, *117*, 187–191. [[CrossRef](#)]
186. Zou, W.; Sun, L.H.; Cong, S.N.; Leng, R.X.; Zhang, Q.; Zhao, L.; Kang, S.Z. Preparation of Worm-like SnS₂ Nanoparticles and Their Photocatalytic Activity. *J. Exp. Nanosci.* **2020**, *15*, 100–108. [[CrossRef](#)]
187. Kgoetlana, C.M.; Malinga, S.P.; Dlamini, L.N. Photocatalytic Degradation of Chlorpyrifos with Mn-WO₃/SnS₂ Heterostructure. *Catalysts* **2020**, *10*, 699. [[CrossRef](#)]
188. Meng, S.; Ogawa, T.; Okumura, H.; Ishihara, K.N. Enhanced Photocatalytic Activity of BiVO₄/Bi₂S₃/SnS₂ Heterojunction under Visible Light. *Catalysts* **2020**, *10*, 1294. [[CrossRef](#)]

189. Fakhri, A.; Behrouz, S.; Pourmand, M. Synthesis, Photocatalytic and Antimicrobial Properties of SnO₂, SnS₂ and SnO₂/SnS₂ Nanostructure. *J. Photochem. Photobiol. B* **2015**, *149*, 45–50. [[CrossRef](#)]
190. Lucena, R.; Fresno, F.; Conesa, J.C. Hydrothermally Synthesized Nanocrystalline Tin Disulphide as Visible Light-Active Photocatalyst: Spectral Response and Stability. *Appl. Catal. A Gen.* **2012**, *415*, 111–117. [[CrossRef](#)]
191. Zhang, Y.C.; Li, J.; Zhang, M.; Dionysiou, D.D. Size-Tunable Hydrothermal Synthesis of SnS₂ Nanocrystals with High Performance in Visible Light-Driven Photocatalytic Reduction of Aqueous Cr(VI). *Environ. Sci. Technol.* **2011**, *45*, 9324–9331. [[CrossRef](#)]
192. Srinivas, B.; Pandit, M.A.; Muralidharan, K. Importance of Clean Surfaces on the Catalyst: SnS₂ Nanorings for Environmental Remediation. *ACS Omega* **2019**, *4*, 14970. [[CrossRef](#)] [[PubMed](#)]
193. Cheraghizade, M.; Jamali-Sheini, F.; Yousefi, R.; Niknia, F.; Mahmoudian, M.R.; Sookhakian, M. The Effect of Tin Sulfide Quantum Dots Size on Photocatalytic and Photovoltaic Performance. *Mater. Chem. Phys.* **2017**, *195*, 187–194. [[CrossRef](#)]
194. Wang, S. Solvothermal Synthesis of Porous SnS₂ Nanotubes with Higher Adsorption and Photocatalytic Activity. *Surf. Sci.* **2019**, *690*, 121469. [[CrossRef](#)]
195. Damkale, S.R.; Arbuj, S.S.; Umarji, G.G.; Panmand, R.P.; Khore, S.K.; Sonawane, R.S.; Rane, S.B.; Kale, B.B. Two-Dimensional Hexagonal SnS₂ Nanostructures for Photocatalytic Hydrogen Generation and Dye Degradation. *Sustain. Energy Fuels*. **2019**, *3*, 3406–3414. [[CrossRef](#)]
196. Sun, Y.; Cheng, H.; Gao, S.; Sun, Z.; Liu, Q.; Leu, Q.; Lei, F.; Yao, T.; He, J.; Wei, S.; et al. Freestanding Tin Disulfide Single-Layers Realizing Efficient Visible-Light Water Splitting. *Angew. Chem. Int. Ed.* **2012**, *51*, 8727–8731. [[CrossRef](#)]
197. Ullah, S.; Bouich, A.; Ullah, H.; Mari, B.; Mollar, M. Comparative Study of Binary Cadmium Sulfide (CdS) and Tin Disulfide (SnS₂) Thin Buffer Layers. *Solar Energy* **2020**, *208*, 637–642. [[CrossRef](#)]
198. Zhang, G.; Du, X.; Wang, Y.; Wang, H.; Wang, W.; Fu, Z. Controllable Synthesis of SnS₂ Nanostructures with High Adsorption and Photocatalytic Activities. *Mater. Sci. Semicond. Process.* **2017**, *64*, 77–84. [[CrossRef](#)]
199. Park, S.; Park, J.; Selvaraj, R.; Kim, Y. Facile Microwave-Assisted Synthesis of SnS₂ Nanoparticles for Visible-Light Responsive Photocatalyst. *J. Ind. Eng. Chem.* **2015**, *31*, 269–275. [[CrossRef](#)]
200. Srivastava, R.R.; Kumar Vishwakarma, P.; Yadav, U.; Rai, S.; Umrao, S.; Giri, R.; Saxena, P.S.; Srivastava, A. 2D SnS₂ Nanostructure-Derived Photocatalytic Degradation of Organic Pollutants Under Visible Light. *Front. Nanotechnol.* **2021**, *3*, 61. [[CrossRef](#)]
201. Zhang, F.; Hou, P.X.; Liu, C.; Wang, B.W.; Jiang, H.; Chen, M.L.; Sun, D.M.; Li, J.C.; Cong, H.T.; Kauppinen, E.I.; et al. Growth of Semiconducting Single-Wall Carbon Nanotubes with a Narrow Band-Gap Distribution. *Nat. Commun.* **2016**, *7*, 11160. [[CrossRef](#)]
202. Dong, R.; Zhong, Y.; Chen, D.; Li, N.; Xu, Q.; Li, H.; He, J.; Lu, J. Morphology-Controlled Fabrication of CNT@MoS₂/SnS₂ Nanotubes for Promoting Photocatalytic Reduction of Aqueous Cr(VI) under Visible Light. *J. Alloys Compd.* **2019**, *784*, 282–292. [[CrossRef](#)]
203. Huang, N.; Liu, J.; Gan, L.; Long, M. Preparation of Size-Tunable SnS₂ Nanocrystals in Situ Adjusted by Nanoporous Graphitic Carbon Nitride in the Process of Hydrothermal Synthesis with Enhanced Photocatalytic Performance. *Mater. Lett.* **2017**, *195*, 224–227. [[CrossRef](#)]
204. Xue, K.; Wang, J.; He, R.; Yang, T.; Yan, Y.; Peng, Y.; Omega, U.; Wang, W. Photoredox Catalysis of As(III) by Constructed -C=Sn-S Bonds: Using Biomass as Templates Leads to Bio-carbon/SnS₂ Nanosheets Capable of the Efficient Photocatalytic Conversion of As(III) and Calcium Arsenate Capture. *Sci. Total Environ.* **2020**, *732*, 138963. [[CrossRef](#)] [[PubMed](#)]
205. Lu, G.; Yu, K.; Wen, Z.; Chen, J. Semiconducting Graphene: Converting Graphene from Semimetal to Semiconductor. *Nanoscale* **2013**, *5*, 1353–1368. [[CrossRef](#)]
206. Yuan, Y.J.; Chen, D.Q.; Shi, X.F.; Tu, J.R.; Hu, B.; Yang, L.X.; Yu, Z.T.; Zou, Z.G. Facile Fabrication of “Green” SnS₂ Quantum Dots/Reduced Graphene Oxide Composites with Enhanced Photocatalytic Performance. *Chem. Eng. J.* **2017**, *313*, 1438–1446. [[CrossRef](#)]
207. Han, L.; Zhong, Y.L.; Lei, K.; Mao, D.; Dong, Y.Z.; Hong, G.; Zhou, Y.T.; Fang, D. Carbon Dot-SnS₂ Heterojunction Photocatalyst for Photoreduction of Cr(VI) under Visible Light: A Combined Experimental and First-Principles DFT Study. *J. Phys. Chem. C* **2019**, *123*, 2398–2409. [[CrossRef](#)]
208. Wang, S.; Li, L.; Zhu, Z.; Zhao, M.; Zhang, L.; Zhang, N.; Wu, Q.; Wang, X.; Li, G. Remarkable Improvement in Photocatalytic Performance for Tannery Wastewater Processing via SnS₂ Modified with N-Doped Carbon Quantum Dots: Synthesis, Characterization, and 4-Nitrophenol-Aided Cr(VI) Photoreduction. *Small* **2019**, *15*, 1804515. [[CrossRef](#)]
209. Huang, R.; Wu, C.; Huang, S.; Chen, D.; Zhang, Q.; Wang, Q.; Hu, Z.; Jiang, Y.; Zhao, B.; Chen, Z. Construction of SnS₂-SnO₂ Heterojunctions Decorated on Graphene Nanosheets with Enhanced Visible-Light Photocatalytic Performance. *Acta Crystallogr. C Struct. Chem.* **2019**, *75*, 812–821. [[CrossRef](#)]
210. Liu, H.; Deng, L.; Zhang, Z.; Guan, J.; Yang, Y.; Zhu, Z. One-Step in-Situ Hydrothermal Synthesis of SnS₂/Reduced Graphene Oxide Nanocomposites with High Performance in Visible Light-Driven Photocatalytic Reduction of Aqueous Cr(VI). *J. Mater. Sci.* **2015**, *50*, 3207–3211. [[CrossRef](#)]
211. Zhong, Y.L.; Han, L.; Yin, X.; Li, H.; Fang, D.; Hong, G. Three Dimensional Functionalized Carbon/Tin(IV) Sulfide Biofoam for Photocatalytic Purification of Chromium(VI)-Containing Wastewater. *ACS Sustain. Chem. Eng.* **2018**, *6*, 10660–10667. [[CrossRef](#)]
212. Raccichini, R.; Varzi, A.; Passerini, S.; Scrosati, B. The Role of Graphene for Electrochemical Energy Storage. *Nat. Mater.* **2015**, *14*, 271–279. [[CrossRef](#)] [[PubMed](#)]
213. Zhu, J.; Duan, R.; Zhang, S.; Jiang, N.; Zhang, Y.; Zhu, J. The Application of Graphene in Lithium Ion Battery Electrode Materials. *J. Korean Phys. Soc.* **2014**, *3*, 585. [[CrossRef](#)] [[PubMed](#)]

214. Sun, Y.; Yang, Y.; Shi, X.L.; Suo, G.; Chen, H.; Noman, M.; Tao, X.; Chen, Z.G. Hierarchical SnS₂/Carbon Nanotube@reduced Graphene Oxide Composite as an Anode for Ultra-Stable Sodium-Ion Batteries. *Chem. Eng. J. Adv.* **2020**, *4*, 100053. [[CrossRef](#)]
215. Sui, D.; Si, L.; Li, C.; Yang, Y.; Zhang, Y.; Yan, W. A Comprehensive Review of Graphene-Based Anode Materials for Lithium-Ion Capacitors. *Chemistry* **2021**, *3*, 1215–1246. [[CrossRef](#)]
216. Wang, G.; Shen, X.; Yao, J.; Park, J. Graphene Nanosheets for Enhanced Lithium Storage in Lithium Ion Batteries. *Carbon. N. Y.* **2009**, *47*, 2049–2053. [[CrossRef](#)]
217. Cui, J.; Yao, S.; Lu, Z.; Huang, J.Q.; Chong, W.G.; Ciucci, F.; Kim, J.K. Revealing Pseudocapacitive Mechanisms of Metal Dichalcogenide SnS₂/Graphene-CNT Aerogels for High-Energy Na Hybrid Capacitors. *Adv. Energy Mater.* **2018**, *8*, 1702488. [[CrossRef](#)]
218. Wang, L.; Zhuo, L.; Yu, Y.; Zhao, F. High-Rate Performance of SnS₂ Nanoplates without Carbon-Coating as Anode Material for Lithium Ion Batteries. *Electrochim. Acta* **2013**, *112*, 439–447. [[CrossRef](#)]
219. Kim, H.S.; Chung, Y.H.; Kang, S.H.; Sung, Y.E. Electrochemical Behavior of Carbon-Coated SnS₂ for Use as the Anode in Lithium-Ion Batteries. *Electrochim. Acta* **2009**, *54*, 3606–3610. [[CrossRef](#)]
220. Guan, S.; Wang, T.; Fu, X.; Fan, L.Z.; Peng, Z. Coherent SnS₂/NiS₂ Hetero-Nanosheet Arrays with Fast Charge Transfer for Enhanced Sodium-Ion Storage. *Appl. Surf. Sci.* **2020**, *508*, 145241. [[CrossRef](#)]
221. Zhou, P.; Wang, X.; Guan, W.; Zhang, D.; Fang, L.; Jiang, Y. SnS₂ Nanowall Arrays toward High-Performance Sodium Storage. *ACS Appl. Mater. Interfaces* **2017**, *9*, 6979–6987. [[CrossRef](#)]
222. Yin, K.; Zhang, M.; Hood, Z.D.; Pan, J.; Meng, Y.S.; Chi, M. Self-Assembled Framework Formed during Lithiation of SnS₂ Nanoplates Revealed by in Situ Electron Microscopy. *Acc Chem. Res.* **2017**, *50*, 1513–1520. [[CrossRef](#)] [[PubMed](#)]
223. Zhang, S. Chemomechanical Modeling of Lithiation-Induced Failure in High-Volume-Change Electrode Materials for Lithium Ion Batteries. *NPJ Comput. Mater.* **2017**, *3*, 7. [[CrossRef](#)]
224. Eom, K.S.; Jung, J.; Lee, J.T.; Lair, V.; Joshi, T.; Lee, S.W.; Lin, Z.; Fuller, T.F. Improved Stability of Nano-Sn Electrode with High-Quality Nano-SEI Formation for Lithium Ion Battery. *Nano. Energy* **2015**, *12*, 314–321. [[CrossRef](#)]
225. Wang, J.; Fan, F.; Liu, Y.; Jungjohann, K.L.; Lee, S.W.; Mao, S.X.; Liu, X.; Zhu, T. Structural Evolution and Pulverization of Tin Nanoparticles during Lithiation-Delithiation Cycling. *J. Electrochem. Soc.* **2014**, *161*, F3019–F3024. [[CrossRef](#)]
226. Demarconnay, L.; Coutanceau, C.; Léger, J.M. Electroreduction of Dioxygen (ORR) in Alkaline Medium on Ag/C and Pt/C Nanostructured Catalysts—Effect of the Presence of Methanol. *Electrochim. Acta* **2004**, *49*, 4513–4521. [[CrossRef](#)]
227. Chia, X.; Lazar, P.; Sofer, Z.; Luxa, J.; Pumera, M. Layered SnS versus SnS₂: Valence and Structural Implications on Electrochemistry and Clean Energy Electrocatalysis. *J. Phys. Chem. C* **2016**, *120*, 24098–24111. [[CrossRef](#)]
228. Yin, L.; Chai, S.; Ma, J.; Huang, J.; Kong, X.; Bai, P.; Liu, Y. Effects of Binders on Electrochemical Properties of the SnS₂ nanostructured Anode of the Lithium-Ion Batteries. *J. Alloys Compd.* **2017**, *698*, 828–834. [[CrossRef](#)]
229. Huang, Y.; Ling, C.; Chen, X.; Zhou, D.; Wang, S. SnS₂ Nanotubes: A Promising Candidate for the Anode Material for Lithium Ion Batteries. *RSC Adv.* **2015**, *5*, 32505–32510. [[CrossRef](#)]
230. Khan, Z.; Parveen, N.; Ansari, S.A.; Senthilkumar, S.T.; Park, S.; Kim, Y.; Cho, M.H.; Ko, H. Three-Dimensional SnS₂ Nanopetals for Hybrid Sodium-Air Batteries. *Electrochim. Acta* **2017**, *257*, 328–334. [[CrossRef](#)]
231. Xia, F.; Yang, F. SnS₂ Monolayer-Supported Transition Metal Atoms as Efficient Bifunctional Oxygen Electrocatalysts: A Theoretical Investigation. *Energy Fuels* **2022**, *36*, 4992–4998. [[CrossRef](#)]
232. Li, J.; Wu, P.; Lou, F.; Zhang, P.; Tang, Y.; Zhou, Y.; Lu, T. Mesoporous Carbon Anchored with SnS₂ Nanosheets as an Advanced Anode for Lithium-Ion Batteries. *Electrochim. Acta* **2013**, *111*, 862–868. [[CrossRef](#)]
233. Liu, Z.; Daali, A.; Xu, G.L.; Zhuang, M.; Zuo, X.; Sun, C.J.; Liu, Y.; Cai, Y.; Hossain, M.D.; Liu, H.; et al. Highly Reversible Sodiation/Desodiation from a Carbon-Sandwiched SnS₂ Nanosheet Anode for Sodium Ion Batteries. *Nano. Lett.* **2020**, *20*, 3844–3851. [[CrossRef](#)] [[PubMed](#)]
234. Xu, Z.; Zhang, Z.; Gao, L.; Lin, H.; Xue, L.; Zhou, Z.; Zhou, J.; Zhuo, S. Tin Disulphide/Nitrogen-Doped Reduced Graphene Oxide/Polyaniline Ternary Nanocomposites with Ultra-High Capacitance Properties for High Rate Performance Supercapacitor. *RSC Adv.* **2018**, *8*, 40252–40260. [[CrossRef](#)] [[PubMed](#)]
235. Ji, L.; Xin, H.L.; Kuykendall, T.R.; Wu, S.L.; Zheng, H.; Rao, M.; Cairns, E.J.; Battaglia, V.; Zhang, Y. SnS₂ Nanoparticle Loaded Graphene Nanocomposites for Superior Energy Storage. *Phys. Chem. Chem. Physics* **2012**, *14*, 6981–6986. [[CrossRef](#)] [[PubMed](#)]
236. Yang, Z.; Zhang, P.; Wang, J.; Yan, Y.; Yu, Y.; Wang, Q.; Liu, M. Hierarchical Carbon@SnS₂ Aerogel with “Skeleton/Skin” Architectures as a High-Capacity, High-Rate Capability and Long Cycle Life Anode for Sodium Ion Storage. *ACS Appl. Mater. Interfaces* **2018**, *10*, 37434–37444. [[CrossRef](#)] [[PubMed](#)]
237. Zhou, N.; Dong, W.D.; Zhang, Y.J.; Wang, D.; Wu, L.; Wang, L.; Hu, Z.Y.; Liu, J.; Mohamed, H.S.H.; Li, Y.; et al. Embedding Tin Disulfide Nanoparticles in Two-Dimensional Porous Carbon Nanosheet Interlayers for Fast-Charging Lithium-Sulfur Batteries. *Sci. China Mater.* **2021**, *64*, 2697–2709. [[CrossRef](#)]
238. Shi, X.; Yang, L.; Li, S.; Wang, Y.; Chen, X.; Wu, Z.; Zhong, Y.; Chen, Y.; Gao, S.; Wang, G.; et al. Promoting Electrochemical Kinetics of Li-S Batteries with C@SnS₂ Modified Separator via Synergic Effect between Porous Carbon Matrix and Polar SnS₂. *Electrochim. Acta* **2021**, *390*, 138829. [[CrossRef](#)]
239. Wei, C.; Han, Y.; Liu, H.; Gan, R.; Li, Q.; Wang, Y.; Hu, P.; Ma, C.; Shi, J. Advanced Lithium-Sulfur Batteries Enabled by a SnS₂-Hollow Carbon Nanofibers Flexible Electrocatalytic Membrane. *Carbon. N. Y.* **2021**, *184*, 11. [[CrossRef](#)]

240. Chang, K.; Wang, Z.; Huang, G.; Li, H.; Chen, W.; Lee, J.Y. Few-Layer SnS₂/Graphene Hybrid with Exceptional Electrochemical Performance as Lithium-Ion Battery Anode. *J. Power Sources* **2012**, *201*, 259–266. [[CrossRef](#)]
241. Du, N.; Wu, X.; Zhai, C.; Zhang, H.; Yang, D. Large-Scale Synthesis and Application of SnS₂-Graphene Nanocomposites as Anode Materials for Lithium-Ion Batteries with Enhanced Cyclic Performance and Reversible Capacity. *J. Alloys Compd.* **2013**, *580*, 457–464. [[CrossRef](#)]
242. Cui, Z.; He, S.; Zhu, J.; Gao, M.; Wang, H.; Zhang, H.; Zou, R. Tailoring the Void Space Using Nanoreactors on Carbon Fibers to Confine SnS₂ Nanosheets for Ultrastable Lithium/Sodium-Ion Batteries. *Small Methods* **2022**, *6*, 2101484. [[CrossRef](#)] [[PubMed](#)]
243. Zhang, Y.; Guo, Y.; Wang, Y.; Peng, T.; Lu, Y.; Luo, R.; Wang, Y.; Liu, X.; Kim, J.K.; Luo, Y. Rational Design of 3D Honeycomb-Like SnS₂ Quantum Dots/RGO Composites as High-Performance Anode Materials for Lithium/Sodium-Ion Batteries. *Nanoscale Res. Lett.* **2018**, *13*, 389. [[CrossRef](#)] [[PubMed](#)]
244. Shi, Y.; Zhou, Y.; Yang, D.R.; Xu, W.X.; Wang, C.; Wang, F.B.; Xu, J.J.; Xia, X.H.; Chen, H.Y. Energy Level Engineering of MoS₂ by Transition-Metal Doping for Accelerating Hydrogen Evolution Reaction. *J. Am. Chem. Soc.* **2017**, *139*, 15479–15485. [[CrossRef](#)]
245. Agarwal, S.; Yu, X.; Manthiram, A. A Pair of Metal Organic Framework (MOF)-Derived Oxygen Reduction Reaction (ORR) and Oxygen Evolution Reaction (OER) Catalysts for Zinc-Air Batteries. *Mater. Today Energy* **2020**, *16*, 100405. [[CrossRef](#)]
246. Kim, S.; Kim, G.; Manthiram, A. A Bifunctional Hybrid Electrocatalyst for Oxygen Reduction and Oxygen Evolution Reactions: Nano-Co₃O₄-Deposited La_{0.5}Sr_{0.5}MnO₃ via Infiltration. *Molecules* **2021**, *26*, 277. [[CrossRef](#)]
247. Zhao, J.; Sarkar, A.; Manthiram, A. Synthesis and Characterization of Pd-Ni Nanoalloy Electrocatalysts for Oxygen Reduction Reaction in Fuel Cells. *Electrochim. Acta* **2010**, *55*, 1756–1765. [[CrossRef](#)]
248. Cheng, Z.; Wang, F.; Shifa, T.A.; Liu, K.; Huang, Y.; Liu, Q.; Jiang, C.; He, J. Carbon Dots Decorated Vertical SnS₂ Nanosheets for Efficient Photocatalytic Oxygen Evolution. *Appl. Phys. Lett.* **2016**, *109*, 053905. [[CrossRef](#)]
249. Chen, T.; Liu, T.; Ding, T.; Pang, B.; Wang, L.; Liu, X.; Shen, X.; Wang, S.; Wu, D.; Liu, D.; et al. Surface Oxygen Injection in Tin Disulfide Nanosheets for Efficient CO₂ Electroreduction to Formate and Syngas. *Nanomicro. Lett.* **2021**, *13*, 189. [[CrossRef](#)]
250. Zhao, Y.; Guo, B.; Yao, Q.; Li, J.; Zhang, J.; Hou, K.; Guan, L. A Rational Microstructure Design of SnS₂-Carbon Composites for Superior Sodium Storage Performance. *Nanoscale* **2018**, *10*, 7999–8008. [[CrossRef](#)]
251. Li, D.; Dai, L.; Ren, X.; Ji, F.; Sun, Q.; Zhang, Y.; Ci, L. Foldable Potassium-Ion Batteries Enabled by Free-Standing and Flexible SnS₂@C Nanofibers. *Energy Environ. Sci.* **2021**, *14*, 424–436. [[CrossRef](#)]
252. He, X.; Liu, J.; Kang, B.; Li, X.; Zeng, L.; Liu, Y.; Qiu, J.; Qian, Q.; Wei, M.; Chen, Q. Preparation of SnS₂/Enteromorpha Prolifera Derived Carbon Composite and Its Performance of Sodium-Ion Batteries. *J. Phys. Chem. Solids* **2021**, *152*, 109976. [[CrossRef](#)]
253. Li, J.; Han, S.; Zhang, C.; Wei, W.; Gu, M.; Meng, L. High-Performance and Reactivation Characteristics of High-Quality, Graphene-Supported SnS₂ Heterojunctions for a Lithium-Ion Battery Anode. *ACS Appl. Mater. Interfaces* **2019**, *11*, 22314–22322. [[CrossRef](#)] [[PubMed](#)]
254. Yin, J.; Cao, H.; Zhou, Z.; Zhang, J.; Qu, M. SnS₂@reduced Graphene Oxide Nanocomposites as Anode Materials with High Capacity for Rechargeable Lithium Ion Batteries. *J. Mater. Chem.* **2012**, *22*, 23963–23970. [[CrossRef](#)]
255. Liu, S.; Yin, X.; Chen, L.; Li, Q.; Wang, T. Synthesis of Self-Assembled 3D Flowerlike SnS₂ Nanostructures with Enhanced Lithium Ion Storage Property. *Solid State. Sci.* **2010**, *12*, 712–718. [[CrossRef](#)]
256. Zhang, Z.; Zhao, H.; Du, Z.; Chang, X.; Zhao, L.; Du, X.; Li, Z.; Teng, Y.; Fang, J.; Świerczek, K. (101) Plane-Oriented SnS₂ Nanoplates with Carbon Coating: A High-Rate and Cycle-Stable Anode Material for Lithium Ion Batteries. *ACS Appl. Mater. Interfaces* **2017**, *9*, 35880–35887. [[CrossRef](#)]
257. Wu, Y.Q.; Zhao, Y.S.; Meng, W.J.; Xie, Y.; Zhang, J.; He, C.J.; Zhao, D.L. Nanoplates-Assembled SnS₂ Nanoflowers with Carbon Coating Anchored on Reduced Graphene Oxide for High Performance Li-Ion Batteries. *Appl. Surf. Sci.* **2021**, *539*, 148283. [[CrossRef](#)]